

Article

Genome-Wide Analysis of the Protein Phosphatase 2C Genes in Tomato

Jianfang Qiu ^{1,2,†}, Lei Ni ^{1,2,†}, Xue Xia ^{1,2}, Shihao Chen ^{1,2}, Yan Zhang ^{1,2}, Min Lang ¹, Mengyu Li ^{1,2}, Binman Liu ^{1,2}, Yu Pan ^{1,2}, Jinhua Li ^{1,2}  and Xingguo Zhang ^{1,2,*}

- ¹ Key Laboratory of Horticulture Science for Southern Mountainous Regions, The Ministry of Education, College of Horticulture and Landscape Architecture, Southwest University, No. 2 Tiansheng Road, Beibei, Chongqing 400715, China; qjf991314@163.com (J.Q.); nl1033148752@163.com (L.N.); xiaxue.tete@outlook.com (X.X.); chenshihao012@163.com (S.C.); zy778865@email.swu.edu.cn (Y.Z.); lang196518@email.swu.edu.cn (M.L.); mengyu151545@163.com (M.L.); swu_liubinman@126.com (B.L.); pany1020@swu.edu.cn (Y.P.); ljh502@swu.edu.cn (J.L.)
- ² State Cultivation Base of Crop Stress Biology for Southern Mountainous Land of Southwest University, Academy of Agricultural Sciences, Southwest University, Beibei, Chongqing 400715, China
- * Correspondence: zhangdupian@swu.edu.cn; Tel.: +86-23-68250974; Fax: +86-23-68251274
- † These authors contributed equally to this work.

Abstract: The plant protein phosphatase 2C (PP2C) plays an irreplaceable role in phytohormone signaling, developmental processes, and manifold stresses. However, information about the PP2C gene family in tomato (*Solanum lycopersicum*) is relatively restricted. In this study, a genome-wide investigation of the SIPP2C gene family was performed. A total of 92 SIPP2C genes were identified, they were distributed on 11 chromosomes, and all the SIPP2C proteins have the type 2C phosphatase domains. Based on phylogenetic analysis of PP2C genes in *Arabidopsis*, rice, and tomato, SIPP2C genes were divided into eight groups, designated A–H, which is also supported by the analyses of gene structures and protein motifs. Gene duplication analysis revealed that the duplication of whole genome and chromosome segments was the main cause of SLPP2Cs expansion. A total of 26 cis-elements related to stress, hormones, and development were identified in the 3 kb upstream region of these SIPP2C genes. Expression profile analysis revealed that the SIPP2C genes display diverse expression patterns in various tomato tissues. Furthermore, we investigated the expression patterns of SIPP2C genes in response to *Ralstonia solanacearum* infection. RNA-seq and qRT-PCR data reveal that nine SIPP2Cs are correlated with *R. solanacearum*. The above evidence hinted that SIPP2C genes play multiple roles in tomato and may contribute to tomato resistance to bacterial wilt. This study obtained here will give an impetus to the understanding of the potential function of SIPP2Cs and lay a solid foundation for tomato breeding and transgenic resistance to plant pathogens.

Keywords: tomato; protein phosphatase 2C; genome-wide; *Ralstonia solanacearum*



Citation: Qiu, J.; Ni, L.; Xia, X.; Chen, S.; Zhang, Y.; Lang, M.; Li, M.; Liu, B.; Pan, Y.; Li, J.; et al. Genome-Wide Analysis of the Protein Phosphatase 2C Genes in Tomato. *Genes* **2022**, *13*, 604. <https://doi.org/10.3390/genes13040604>

Academic Editor: Abdelhafid Bendahmane

Received: 5 March 2022

Accepted: 24 March 2022

Published: 28 March 2022

Publisher's Note: MDPI stays neutral with regard to jurisdictional claims in published maps and institutional affiliations.



Copyright: © 2022 by the authors. Licensee MDPI, Basel, Switzerland. This article is an open access article distributed under the terms and conditions of the Creative Commons Attribution (CC BY) license (<https://creativecommons.org/licenses/by/4.0/>).

1. Introduction

Plants may inevitably encounter many kinds of unpredictable environmental challenges, such as pathogen infection, extreme temperature, salt, and drought, which will adversely affect their growth, development, and production [1]. To adapt to these adversities, plants have evolved signaling mechanisms to deliver stimuli to different cellular compartments and then feedback to these stresses. Protein kinases (PKs) and protein phosphatases (PPs) modulate the protein function by reversible protein phosphorylation mechanism and are known to play a vital role in pivotal stress signaling processes [2]. In the past years, several PKs had been massively investigated and proved to be positive regulation factors responding to a variety of stresses [3–6]. On the contrary, PPs have not been studied as extensively as PKs.

PPs can remove phosphate groups from phosphorylated proteins through their special structure and can change protein function to respond to external pressure [7]. They

are categorized into three major classes: tyrosine phosphatases (PTPs), serine/threonine phosphatases (PSPs), and dual-specificity phosphatases (DSPTPs), which is determined by the specificity of a substrate [8]. Moreover, PSPs are further classified into phospho-protein phosphatases (PPP) and phosphoprotein metallophosphatase (PPM) based on distinct amino acid sequences, different dependencies on metal ions, and sensitivities to inhibitors [9]. PP1, PP2A, PP2B, PP4, PP5, PP6, and PP7 were included in the PPP family, whereas the PPM family is represented by PP2C and others [8,10,11].

Due to the special differences between amino acid and crystal structure, PP2C proteins require metal ion Mg^{2+} or Mn^{2+} to accomplish their function [12]. In eukaryotes, the catalytic domain of PP2C proteins is located at either the N-terminus or the C-terminus. Further research revealed that the regions of the catalytic domain in eukaryotic PP2C proteins are relatively conserved, whereas the regions of a non-catalytic domain have diverse amino acid sequences [13]. PP2Cs are quite conserved in evolution from prokaryotes to higher eukaryotes, having been found in archaea, bacteria, fungi, plants, and animals, significantly modulate stress signaling pathways, and reverse the stress-induced PK cascades in response to environmental stimuli [14]. In plants, PP2Cs form the largest family of phosphatase genes, accounting for 60–65% of all phosphorylases [8,15]. The high proportion of PP2C genes in plants indicates their evolutionary significance, requirement, and participation in varying plant cellular functions [10]. As a major class of protein phosphatases, PP2Cs catalyze the dephosphorylation of substrate proteins to regulate signaling pathways and participate in various physiological and biochemical processes in plants. Current studies have indicated that PP2Cs play important regulatory roles in different processes, such as ABA signaling, biotic and abiotic stress responses, plant immunity, K^+ nutrient signaling, and plant development [8,10,13–17]. There were extensive studies on the role of PP2C proteins. For example, *PpABI1A* and *PpABI1B* in moss are directly involved in ABA responses [18]. In higher plants, the function of PP2Cs is more diverse, among which PP2Cs in group A is the most intensively studied. In *Arabidopsis thaliana*, the PP2Cs of group A, well-studied as ABA co-receptors, negatively regulate the ABA signaling pathway. For instance, *ABI1*, *ABI2*, and *HAB1* participate in plant abiotic stress by negatively regulating ABA signaling and *ABI1* plays a negative regulatory role in response to ABA-mediated drought stress [19–21]. In tomato, *SIPP2C1*, an *ABI2* homology, negatively regulates ABA signaling and fruit ripening. *SIPP2C1-RNAi* led to increased endogenous ABA accumulation and advanced release of ethylene in transgenic fruit compared with wild-type (WT) fruit. *SIPP2C1-RNAi* plants were hypersensitized to ABA and displayed delayed seed germination and primary root growth, and increased resistance to drought stress compared with WT control plants [22]. In maize, *ZmPP2C-A10* is tightly associated with drought tolerance, and similar to its *Arabidopsis* orthologs, it interacts with *ZmPYL* ABA receptors and *ZmSnRK2* protein kinases, suggesting that *ZmPP2C-A10* is involved in mediating ABA signaling. Transgenic studies confirmed that *ZmPP2C-A10* functions as a negative regulator of drought tolerance [23]. Similar results have been obtained from poplar [24] and sweet cherry [25] studies. On the contrary, in *Brachypodium distachyon*, *BdPP2CA6*, a member of group A of PP2C, was found to be a positive regulator in both ABA and stress signaling pathways [26]. These studies indicate that the PP2Cs of group A have diverse functions in different plants. In *Arabidopsis*, the PP2Cs of group B function as mitogen-activated protein kinase (MAPK) phosphatases. *AtAP2C1* regulates phytohormone and defense responses by cooperating with MPK4 and MPK6 [27–29], whereas *AtAP2C3* mediates stomata development; thus, negatively regulating MAPK signaling [30]. Group D comprises nine PP2Cs in *Arabidopsis*, all of which have different expression patterns and subcellular localization [31]. In group E, *AtPP2C-6-6* interacts with histone acetyltransferase (*AtGCN5*) to control the activation of stress-responsive genes in the stomatal signaling network. In group F, *AtWIN2* may interact with the bacterial effector *HopW1-1* and regulates *HopW1-1* to induce disease response [32]. These studies indicate that PP2Cs have diverse functions worth investigating.

To date, there are 80, 78, 257, 62, and 131 genes coding for PP2C proteins identified using bioinformatics surveys in Arabidopsis, rice [33], wheat [34], woodland strawberry [35], and *Brassica rapa* [36], respectively. The studies mentioned above have proved the diverse roles of PP2C genes. Hence, it is necessary to delve into the comprehension and functional characterization of the PP2C gene family.

Tomato is one of the most consumed vegetables in the world, and its annual output has reached 181 million tons (Food and Agriculture Organization of the United Nations, <http://www.fao.org/> (accessed on 5 March 2022)). Tomato and its derivatives have become an indispensable part of daily life. *Ralstonia solanacearum*, previously known as *Pseudomonas solanacearum*, is internationally recognized as one of the leading models in the analysis of plant pathogenicity. This soil bacterium is a severe and devastating disease of solanaceous crops (<https://iant.toulouse.inra.fr/R.solanacearum> (accessed on 5 March 2022)). Tomato genome sequencing has been completed (<https://solgenomics.net> (accessed on 5 March 2022)), but the tomato PP2C family genetic research in plant pathogen, *R. solanacearum*, remains unknown. In this study, bioinformatics analysis of tomato PP2C gene family members was conducted to preliminarily explore the expression characteristics and response rules of this gene family in tomato which were infected with *R. solanacearum*. In our study, 92 SIPP2Cs were identified, and their physical and chemical properties, subcellular localization, exon–intron structure, phylogenetic comparison, gene duplication, chromosome distribution, and cis-acting elements were analyzed. SIPP2Cs under *R. solanacearum* infection were also examined. Our results were a reliable prediction for the function and structure of SIPP2Cs, which would provide a solid basis for performing further functional analysis of these genes.

2. Materials and Methods

2.1. Identification of SIPP2C Members

To gain the whole SIPP2C genes of tomato, genome data of ITAG 4.0 were downloaded from Phytozome (<http://phytozome.jgi.doe.gov/pz/portal.html> (accessed on 5 March 2022)) [37] to set up a local database, and seed file of the SIPP2C protein domain (PF00481) [38] was downloaded from the Pfam (<http://pfam.xfam.org/> (accessed on 5 March 2022)) [39]. The HMMER [40] procedures of hmm build and hmm search were fully used to retrieve all assumed SIPP2C sequences with default parameters in tomato and the ID of the relevant sequences was collected (E-value < 1.0). The ID was submitted to the SGN (<http://solgenomics.net/> (accessed on 5 March 2022)) [41] to eliminate the sequence that shows no difference in their amino acid. After manually removing the redundant sequences, all these predicted genes were examined in SMART (<http://smart.embl-heidelberg.de/> (accessed on 5 March 2022)) [42] and CDD (<https://www.ncbi.nlm.nih.gov/cdd> (accessed on 5 March 2022)) [43]. Protein physicochemical properties and subcellular localization of SIPP2Cs were calculated by the online software ExPASy (<https://www.expasy.org/> (accessed on 5 March 2022)) [44] and Cell-PLoc 2 (<http://www.csbio.sjtu.edu.cn/bioinf/plant-multi/> (accessed on 5 March 2022)) [45]. The chromosome length of tomato and the location data of each SIPP2C gene were retrieved from SGN.

2.2. Phylogenetic Analysis

Validated tomato PP2C protein sequences were employed for establishing an evolutionary relationship with the known PP2C members of Arabidopsis (*AtPP2Cs*) and *Oryza sativa* (*OsPP2Cs*) [33]. This analysis included 250 amino acid sequences. ClustalW [46] was used to conduct multiple sequence alignment. Ground on the outcomes of aa sequence alignment, the maximum likelihood method in MEGA-X [47] was used to design the phylogenetic tree with default parameters. The Blast program was applied to discern tandem repeat genes. If the identity between two genes was more than 75% and the alignment length was more than 75% of the longer sequence, they were considered to be tandem

repeat gene pairs [48]. *Ka/Ks* of all *SIPP2C* tandem repeat gene pairs was calculated using *KaKs_Calculator* [49]. The relationship of tandem repeats was displayed via *TBtools* [50].

2.3. Chromosomal Location, Gene Structure, and Sequence Alignment

The *PP2C* genes were mapped to tomato chromosomes by identifying their chromosomal positions according to the SGN database. The proportion chart of the chromosomal location was drawn using *TBtools*. The exon and intron structures of *SIPP2Cs* were generated using the Gene Structure Display Server 2.0 (<http://gsds.cbi.pku.edu.cn> (accessed on 5 March 2022)) [51] by aligning the CDS sequences with the corresponding genomic DNA sequences from the SGN database. Domains were confirmed using the Pfam and the SMART programs.

2.4. Cis-Element Prediction for *PP2C* Gene Promoter

It is well known that most of the functional cis-active elements in vivo (about 80%) are concentrated in the proximal promoter [52]. However, how to determine the boundary of the promoter region has not been determined. Generally speaking, 1 kb, 2 kb, or longer upstream of ATG is taken. Therefore, the aim of this paper was to take 3 kb. The promoter sequence (3 kb upstream of the putative genes ATG) was extracted from the ITAG 4.0 gff3 file. All the promoter sequences were uploaded to the PlantCARE database (<http://bioinformatics.psb.ugent.be/webtools/plantcare/html/> (accessed on 5 March 2022)) [53] for cis-element prediction. The result was visualized with *TBtools*.

2.5. Expression Analysis of *SIPP2Cs* of Tomato Tissue

RNA-seq data from the platform TFGD (Tomato Functional Genomics Database) (<http://ted.bti.cornell.edu/> (accessed on 5 March 2022)) [54] played a part in the expression patterns of *SIPP2Cs*. The data included reads from the Illumina RNA-seq analysis of leaves, roots, flower buds, fully opened flowers, and 1, 2, and 3 cm, mature green, breaker, and breaker +10 fruit of the tomato cultivar Heinz. Gene expression level was defined on the basis of the normalized expression value, that is, reads per kilobases per million (RPKM) for each tissue/stage. The \log_2 logarithmic transformation of the RPKM values was selected from the platform, and heat maps were plotted to analyze their expression levels.

2.6. Transcriptional Profiling of *SIPP2C* Genes in Tomato Infected with *Ralstonia solanacearum*

RNA-seq data from our laboratory (unpublished data) were performed to gain insight into the expression profiles of the *SIPP2C* gene families under *R. solanacearum* infection. Gene expression level was defined on the basis of the normalized expression value, that is, reads per kilobases per million (RPKM) for each sample. The \log_2 logarithmic transformation of the RPKM values was selected, and heat maps were plotted to analyze their expression levels. The expression values of *SIPP2C* genes that were upregulated or downregulated by more than two-fold with $p < 0.05$ were considered as differentially expressed.

2.7. Bacterial Strain of *Ralstonia solanacearum*

The standard strain GMI1000 of *R. solanacearum* was used to infect tomato stems. The tested pathogen GMI1000 was grown on solid TTC medium plates for 3 days at 28 °C; then inoculated in liquid TTC medium to grow overnight at 28 °C [55]. Then, 100 μ L overnight bacterial solution was absorbed into TTC liquid medium and activated for 24 h at 28 °C, which can be used for the inoculation test.

2.8. Plant Material and Treatments

The germinated seeds of tomato were grown in plastic pots containing a mixture of soil and vermiculite (3:1). The pots were then placed in greenhouse with a 16 h light/8 h dark cycle photoperiod, and the temperature was 25 ± 2 °C. The humidity was maintained at approximately 60–70%, and the photosynthetic photon flux density was controlled at about 120 μ mol photons/ m^2 /s. When the seedlings were six weeks old, the plants were

used in the inoculation experiment. Untreated plants were used as controls to avoid the effects of biological clock on differential gene expression. Specific treatments were provided to the seedlings as follows: The stem of selected tomato plants was needled with 1 mL of activated bacterial solution and cultured in an artificial climate chamber with 28 °C for 3 days. After 3 days of treatment, the materials of stems were immediately frozen in liquid nitrogen and then stored at −80 °C until use.

2.9. RNA Isolation and Real-Time PCR

A total of 100 µL of RNA was extracted using the Total RNA Kit (BioTeke Corporation, Beijing, China), following the manufacturer's instructions. The integrity of the RNA was verified by agarose gel electrophoresis. Synthesis of the cDNA was performed from the total RNA samples using the PrimeScript™ RT Reagent Kit, according to the protocol with gDNA Eraser (TaKaRa, Dalian, China). Specific primers were designed using qPrimerDB [56] and are presented in Supplementary Table S1. The *SIELF-α* gene was used as the internal control [57] to quantitate the expression of *SIPP2C* genes. Real-time PCR was performed using CFX96 Touch™ Real-time PCR System (Bio-Rad, Hercules, CA, USA) with a SYBR Premix Ex Taq™ II Kit (Bio-Rad). The reactions were carried out in the following conditions: denaturation at 94 °C for 4 min, 40 cycles of 5 s at 95 °C, 30 s at 60 °C, 15 s at 95 °C, 20 s at 60 °C, and 15 s at 95 °C. Three biological duplications were used. The $2^{-\Delta\Delta C_t}$ method was used to analyze the real-time PCR data [58]. Relative expressions were visualized using Graphpad Prism [59].

3. Results

3.1. Identification of PP2C Genes in Tomato

To identify the *PP2C* genes in the tomato, we searched for sequences that contained the particular domain in the tomato protein database using the hidden Markov model (HMM) model of PF00481 and confirmed the presence of *PP2C* domains using Pfam and Batch CD-search and found 92 *PP2C* genes (Supplementary Table S2). These genes were labeled as *SIPP2C01* to *SIPP2C92* on the basis of their distributions and relative linear orders among their respective chromosomes. The information of gene ID, the amino acid (aa) length, isoelectric point (pI), molecular weight (Mw), hydrophilic coefficient, instability index, and subcellular localization prediction of 92 *PP2C* proteins were analyzed (Table 1). The lengths of proteins varied from 59 aa residues (*SIPP2C62*) to 1080 aa residues (*SIPP2C37*), with an average length of 190 aa. Most of the lengths of the *PP2C* proteins were between 300 and 400 aa. The pI varied from 4.62 (*SIPP2C90*) to 11.39 (*SIPP2C08*) and Mw ranged from 6738.81Da (*SIPP2C62*) to 119917.55Da (*SIPP2C37*). The result of hydropathicity (GRAVY) showed that *SIPP2Cs* except for *SIPP2C92* were hydrophilic proteins. The result of the instability index proclaimed that 67.4% *SIPP2Cs* were unstable proteins. The result of subcellular localization prediction showed that most tomato *PP2C* proteins were predicted to be in the intracellular (97.8%), such as the cytoplasm, chloroplast, mitochondrion, nucleus, and peroxisome, but some proteins may be located in extracellular or cell membrane (2.1%). These results revealed that *SIPP2C* proteins were organelle-specific and had a function in various environments.

Table 1. Information of the protein phosphatase 2C (*PP2C*) gene family in tomato.

Gene	Identifier	Chromosome		AA	PIs/MW	GRAVY	Instability	Subcellular
		Location					Index	Localization
<i>SIPP2C01</i>	Solyc01g065700.3.1	chr01:	72,289,658–72,295,088	361	6.47/39,992.45	−0.266	35.78	Cyto
<i>SIPP2C02</i>	Solyc01g066870.3.1	chr01:	750,92,877–75,095,866	522	5.09/57,125.35	−0.202	42.69	Cyto
<i>SIPP2C03</i>	Solyc01g067980.1.1	chr01:	77,027,259–77,032,781	202	6.19/20,650.27	−0.001	31.43	Extr. Nucl
<i>SIPP2C04</i>	Solyc01g068000.4.1	chr01:	77,050,710–77,057,722	297	4.89/32,913.15	−0.202	54.88	Nucl
<i>SIPP2C05</i>	Solyc01g079720.3.1	chr01:	78,822,308–78,843,121	613	6/68,185.28	−0.282	45.77	Cyto
<i>SIPP2C06</i>	Solyc01g080400.3.1	chr01:	79,645,915–79,653,551	414	4.81/45,150.79	−0.406	46.18	Nucl
<i>SIPP2C07</i>	Solyc01g087460.3.1	chr01:	82,424,646–82,428,543	372	6.17/41,583.98	−0.655	38.39	Nuc

Table 1. Cont.

Gene	Identifier	Chromosome		AA	PIs/MW	GRAVY	Instability		Subcellular	
		Location					Index	Localization		
SIPP2C08	Solyc01g094230.4.1	chr01:	85,781,740–85,791,508	627	11.39/64,450.04	−0.476	35.66		Nucl	
SIPP2C09	Solyc01g100040.3.1	chr01:	90,110,898–90,115,136	367	6.22/40,919.44	−0.258	38.73		Nucl	
SIPP2C10	Solyc01g100110.4.1	chr01:	90,196,815–90,202,470	427	6.91/46,135.74	−0.146	43.86		Cyto. Nucl	
SIPP2C11	Solyc01g105280.3.1	chr01:	93,506,692–93,513,168	283	6.8/30,954.82	−0.426	36.53		Cyto. Nuc	
SIPP2C12	Solyc01g107300.4.1	chr01:	94,888,760–94,892,503	278	7.79/31,335.87	−0.128	46.13		Cyto	
SIPP2C13	Solyc01g111730.3.1	chr01:	97,915,696–97,923,710	388	8.23/42,809.56	−0.263	44.55		Chlo. Nucl	
SIPP2C14	Solyc02g082490.4.1	chr02:	46,189,450–46,193,937	384	5.67/41,815.49	−0.313	50.46		Nucl	
SIPP2C15	Solyc02g083420.3.1	chr02:	46,831,821–46,836,739	390	7.74/43,034.89	−0.226	48.53		Nucl	
SIPP2C16	Solyc02g092730.3.1	chr02:	53,716,175–53,721,010	366	5.45/40,529.01	−0.229	39.32		Nucl	
SIPP2C17	Solyc03g006930.3.1	chr03:	1,502,552–1,506,122	331	6.09/36,843.85	−0.25	59.95		Cyto	
SIPP2C18	Solyc03g006940.3.1	chr03:	1,509,616–1,512,540	345	4.95/37,872.93	−0.185	57		Nucl	
SIPP2C19	Solyc03g006950.3.1	chr03:	1,514,383–1,518,178	347	6.02/38,049.53	−0.147	53.69		Nucl	
SIPP2C20	Solyc03g006960.4.1	chr03:	1,519,421–1,523,583	304	5.7/33,397.94	−0.255	56.99		Cyto	
SIPP2C21	Solyc03g007230.4.1	chr03:	1,791,778–1,795,346	397	5.72/43,979.53	−0.424	50.8		Nucl	
SIPP2C22	Solyc03g007270.3.1	chr03:	1,828,441–1,838,542	299	4.96/32,489.18	−0.432	43.54		Nucl	
SIPP2C23	Solyc03g013100.1.1	chr03:	47,516,649–47,518,201	114	6.51/12,939.8	−0.337	35.03		Mito	
SIPP2C24	Solyc03g013140.1.1	chr03:	47,332,347–47,334,696	163	5.81/18,565.16	−0.428	20.18		Cyto	
SIPP2C25	Solyc03g033340.3.1	chr03:	4,912,004–4,918,389	397	7.65/43,970.18	−0.217	47.54		Chlo. Nucl	
SIPP2C26	Solyc03g065190.1.1	chr03:	40,216,058–40,218,346	123	9.55/14,453	−0.293	32.52		Cyto. Extr. Nucl	
SIPP2C27	Solyc03g082960.2.1	chr03:	52,814,842–52,820,023	395	6.29/43,427.5	−0.203	44.71		Nucl	
SIPP2C28	Solyc03g096670.3.1	chr03:	58,989,562–58,992,297	406	6/44,683.73	−0.397	52.59		Cyto. Nucl	
SIPP2C29	Solyc03g118890.4.1	chr03:	67,672,668–67,679,525	329	6.22/36,093.73	−0.248	42.26		Cyto	
SIPP2C30	Solyc03g121880.4.1	chr03:	69,911,090–69,918,573	548	5.86/59,716.58	−0.095	38.86		Cyto	
SIPP2C31	Solyc04g056560.4.1	chr04:	54,528,741–54,538,177	401	4.87/43,785.08	−0.266	32.37		Nucl	
SIPP2C32	Solyc04g064500.4.1	chr04:	55,645,130–55,673,295	372	4.95/40,544.4	−0.481	45.68		Nucl	
SIPP2C33	Solyc04g074190.3.1	chr04:	60,189,483–60,198,295	278	6.32/30,483.44	−0.345	49.68		Cyto. Nucl	
SIPP2C34	Solyc04g079120.3.1	chr04:	63,704,094–63,711,682	428	5.28/46,166.21	−0.296	47.94		Nucl	
SIPP2C35	Solyc04g082600.3.1	chr04:	66,227,666–66,234,622	387	4.85/42,607.25	−0.265	47.37		Chlo. Nucl	
SIPP2C36	Solyc05g009070.4.1	chr05:	3,216,982–3,221,083	339	8.01/37,083.37	−0.231	35.43		Nucl	
SIPP2C37	Solyc05g018300.3.1	chr05:	20,358,675–20,387,085	1080	4.81/119,917.55	−0.203	42.53		Nucl	
SIPP2C38	Solyc05g052520.3.1	chr05:	62,745,936–62,749,176	396	5.56/42,845.56	−0.233	53.55		Nucl	
SIPP2C39	Solyc05g052980.4.1	chr05:	63,149,350–63,151,994	437	5.69/48,147.65	−0.281	52.66		Nucl	
SIPP2C40	Solyc05g053290.3.1	chr05:	63,421,852–63,425,476	411	4.73/44,751.23	−0.109	43.03		Nucl	
SIPP2C41	Solyc05g055790.4.1	chr05:	65,291,032–65,295,556	499	5.23/55,284.13	−0.375	52.06		Nucl	
SIPP2C42	Solyc05g055980.4.1	chr05:	65,383,352–65,389,926	314	6.91/35,158.87	−0.366	43.45		Chlo. Nucl	
SIPP2C43	Solyc06g007190.4.1	chr06:	1,265,243–1,268,111	412	7.97/4,4889.01	−0.182	44.84		Nucl	
SIPP2C44	Solyc06g009390.3.1	chr06:	3,311,448–3,316,710	352	4.94/38,881.06	−0.11	56.6		Nucl	
SIPP2C45	Solyc06g051940.4.1	chr06:	35,603,081–35,605,882	471	5.8/51,885.49	−0.36	43.54		Nucl	
SIPP2C46	Solyc06g065610.3.1	chr06:	40,985,604–40,992,533	375	5.59/40,805.91	−0.342	45.11		Nucl	
SIPP2C47	Solyc06g065920.4.1	chr06:	41,312,022–41,318,633	374	8.51/41,712.42	−0.298	46.39		Nucl	
SIPP2C48	Solyc06g076100.3.1	chr06:	47,243,874–47,248,381	708	5.41/79,199.49	−0.537	38.2		Nucl	
SIPP2C49	Solyc06g076400.3.1	chr06:	47,471,880–47,474,601	410	5.12/44,859.67	−0.346	46.42		Nucl	
SIPP2C50	Solyc06g082080.3.1	chr06:	48,014,366–48,017,179	379	8.18/40,564.02	−0.241	52.55		Nucl	
SIPP2C51	Solyc06g082700.1.1	chr06:	48,429,677–48,430,277	142	6.09/15,813.08	−0.125	26.13		Cell membrane. Chlo. Cyto	
SIPP2C52	Solyc07g007220.3.1	chr07:	1,956,469–1,961,556	383	5.07/42,272.7	−0.264	47.32		Nucl	
SIPP2C53	Solyc07g024010.2.1	chr07:	23,836,770–23,838,030	136	6.07/15,409.59	−0.258	24.63		Chlo	
SIPP2C54	Solyc07g024020.2.1	chr07:	23,848,754–23,851,910	321	5.09/34,819.28	−0.321	40.61		Nucl	
SIPP2C55	Solyc07g040990.4.1	chr07:	51,484,565–51,489,081	536	5.38/59,196.43	−0.267	47.81		Nucl	
SIPP2C56	Solyc07g053760.4.1	chr07:	62,192,070–62,195,463	286	6.67/31,303.63	−0.331	37.81		Nucl	
SIPP2C57	Solyc07g054300.3.1	chr07:	62,654,289–62,659,599	478	5.38/53,166.78	−0.45	44.34		Nucl	
SIPP2C58	Solyc07g062970.3.1	chr07:	65,595,765–65,600,127	282	5.67/30,943.93	−0.327	28.7		Nucl	
SIPP2C59	Solyc07g066260.3.1	chr07:	67,742,920–67,748,833	515	5.75/56,463.59	−0.371	38.51		Chlo. Nucl	
SIPP2C60	Solyc08g006660.3.1	chr08:	803,615–827,195	368	4.99/40,229.15	−0.398	38.43		Nucl	
SIPP2C61	Solyc08g007000.3.1	chr08:	1,574,889–1,583,560	781	5.23/86,116.34	−0.491	47.03		Chlo	
SIPP2C62	Solyc08g044610.3.1	chr08:	18,794,957–18,799,764	59	6.71/6738.81	0.012	42.27		Chlo. Nucl.	
SIPP2C63	Solyc08g062640.3.1	chr08:	51,623,577–51,625,677	134	7.61/15,444.01	−0.244	40.43		Nucl.	
SIPP2C64	Solyc08g062650.2.1	chr08:	51,624,426–51,632,488	469	4.89/51,638.63	−0.057	38.97		Nucl	
SIPP2C65	Solyc08g065500.2.1	chr08:	53,632,222–53,634,431	336	5.06/36,816.81	−0.137	40.85		Nucl	
SIPP2C66	Solyc08g065540.3.1	chr08:	53,677,271–53,679,628	332	5.59/36,782.71	−0.185	39.99		Nucl	
SIPP2C67	Solyc08g065670.4.1	chr08:	53,898,474–53,901,007	306	5.22/33,454.16	−0.075	40.12		Nucl	
SIPP2C68	Solyc08g065680.3.1	chr08:	53,924,816–53,927,725	205	5.24/22,537.35	−0.166	44.21		Nucl	
SIPP2C69	Solyc08g074230.1.1	chr08:	58,350,631–58,355,073	271	4.76/30,183.9	−0.518	37.99		Nucl	
SIPP2C70	Solyc08g077150.3.1	chr08:	61,046,865–61,055,706	796	5.19/87,391.85	−0.456	50.57		Chlo	
SIPP2C71	Solyc08g082260.2.1	chr08:	65,099,205–65,101,710	393	6.17/44,173.95	−0.55	45.52		Nucl	

Table 1. Cont.

Gene	Identifier	Chromosome		AA	PIs/MW	GRAVY	Instability		Subcellular	
		Location					Index	Localization		
SIPP2C72	Solyc09g007080.3.1	chr09: 727,617–731,731		378	9.06/41,932.11	−0.266	41.45	Chlo. Cyto. Mito. Nucl		
SIPP2C73	Solyc09g010780.3.1	chr09: 4,070,320–4,073,958		623	5.4/69,387.69	−0.394	29.6	Chlo		
SIPP2C74	Solyc09g065650.3.1	chr09: 63,821,833–63,855,480		955	5.43/109,110.03	−0.408	38.77	Nucl		
SIPP2C75	Solyc09g090280.3.1	chr09: 69,809,431–69,813,531		257	9.78/28,883.02	−0.807	42.35	Chlo. Nucl		
SIPP2C76	Solyc10g005640.4.1	chr10: 513,071–520,386		556	5.56/61,356.83	−0.502	41.89	Nucl		
SIPP2C77	Solyc10g008490.3.1	chr10: 2,617,430–2,620,523		469	5.02/51,815.01	−0.455	46.09	Nucl		
SIPP2C78	Solyc10g047290.2.1	chr10: 40,367,471–40,374,422		281	8.32/30,574.56	−0.431	40.11	Nucl		
SIPP2C79	Solyc10g049630.2.1	chr10: 46,299,689–46,303,378		381	9.06/42,379.44	−0.334	48.38	Nucl		
SIPP2C80	Solyc10g055650.2.1	chr10: 57,152,293–57,156,799		388	8.67/43,047.9	−0.271	42.35	Nucl. Pero		
SIPP2C81	Solyc10g076320.3.1	chr10: 59,239,617–59,243,965		344	6.05/38,842.14	−0.424	40.32	Chlo. Nucl		
SIPP2C82	Solyc10g078800.3.1	chr10: 60,493,362–60,504,498		947	5.26/105,611.28	−0.386	45.49	Nucl		
SIPP2C83	Solyc10g078810.1.1	chr10: 60,504,641–60,507,279		438	4.93/48,492.24	−0.355	39.39	Nucl		
SIPP2C84	Solyc10g078820.2.1	chr10: 60,508,870–60,512,342		460	4.99/51,210.32	−0.422	46.42	Nucl		
SIPP2C85	Solyc10g084410.2.1	chr10: 63,960,722–63,963,486		376	9.42/41,906.86	−0.346	47.56	Nucl		
SIPP2C86	Solyc10g085370.3.1	chr10: 64,570,827–64,575,317		453	5.86/51,847.37	−0.654	36.8	Nucl		
SIPP2C87	Solyc10g086490.2.1	chr10: 65,295,550–65,298,502		596	5.67/66,435.52	−0.392	39	Cell membrane. Chlo		
SIPP2C88	Solyc12g010450.3.1	chr12: 3,470,481–3,476,558		316	5.75/34,814.63	−0.272	43.32	Cyto		
SIPP2C89	Solyc12g042570.2.1	chr12: 39,939,943–39,959,306		362	4.92/39,315.91	−0.512	39.46	Nucl		
SIPP2C90	Solyc12g096020.3.1	chr12: 65,098,300–65,101,758		508	4.62/55,681.53	−0.235	45.3	Nucl		
SIPP2C91	Solyc12g096520.3.1	chr12: 65,400,452–65,408,533		293	5.04/31,552.91	−0.349	34.47	Cyto		
SIPP2C92	Solyc12g099600.2.1	chr12: 66,688,468–66,694,648		497	5.35/53,856.74	−0.189	47.82	Nucl		

AA: number of amino acids; pIs: theoretical isoelectric point; MW: molecular weight (kDa). GRAVY: grand average of hydropathicity (GRAVY < 0, hydrophilic protein/GRAVY > 0, hydrophobic protein), Instability Index (<40, the protein is stable/>40, the protein is unstable). Cyto: cytoplasm; Extr: extracellular; Nucl: nucleus; Chlo: chloroplast; Mito: mitochondria; Pero: peroxisome.

3.2. Phylogenetic and Comparative Synteny Analysis

To gain insights into the evolutionary relationship within the *PP2C* gene family in Arabidopsis, rice, and tomato, an unrooted phylogenetic tree was structured with the amino acid of 78 *OsPP2Cs* of rice, 80 *AtPP2Cs* of Arabidopsis, and 92 *SIPP2Cs* of tomato using the MEGA-X by the adopting maximum likelihood (ML) approach (Supplementary Table S3). The findings of the phylogenetic tree depicted that *PP2C* genes were further divided into eight groups, labeled from A to H, which was also supported by the analyses of *SIPP2Cs* gene structures and protein motifs. Group F is the largest, with 49 members, while group E is the smallest, with only 14 members (Figure 1, Table 2). The *SIPP2Cs* showed a species-specific evolutionary classification.

Table 2. The distribution of *PP2C* genes in Arabidopsis, rice, and tomato.

Subgroup of <i>PP2C</i> Genes	Numbers of <i>AtPP2Cs</i>	Numbers of <i>OsPP2Cs</i>	Numbers of <i>SIPP2Cs</i>
A	9	9	15
B	8	18	12
C	9	8	11
D	13	11	11
E	6	3	5
F	19	14	16
G	7	5	8
H	9	10	14

AtPP2Cs: Arabidopsis thaliana *PP2Cs*; *OsPP2Cs*: Oryza sativa *PP2Cs*; *SIPP2Cs*: Solanum lycopersicum *PP2Cs*.

To better understand the difference in evolution and replication events involved in the *PP2C* gene family, the collinear relationship was analyzed in *PP2C* genes from tomato, rice, and Arabidopsis. The result showed that a total of 63 *PP2C* members participated in the synteny relationship (Figure 2, Supplementary Table S4). There are 17, 9, and 3 gene pairs represented as collinear in tomato, Arabidopsis, and rice, respectively, and the number of

collinear gene pairs between tomato and rice, tomato and Arabidopsis, rice and Arabidopsis were 6, 12, and 5 pairs separately, which showed that *PP2C* genes of tomato, rice, and Arabidopsis reflected more diversity in evolution, and the number of homologous genes was relatively less (Supplementary Table S5).

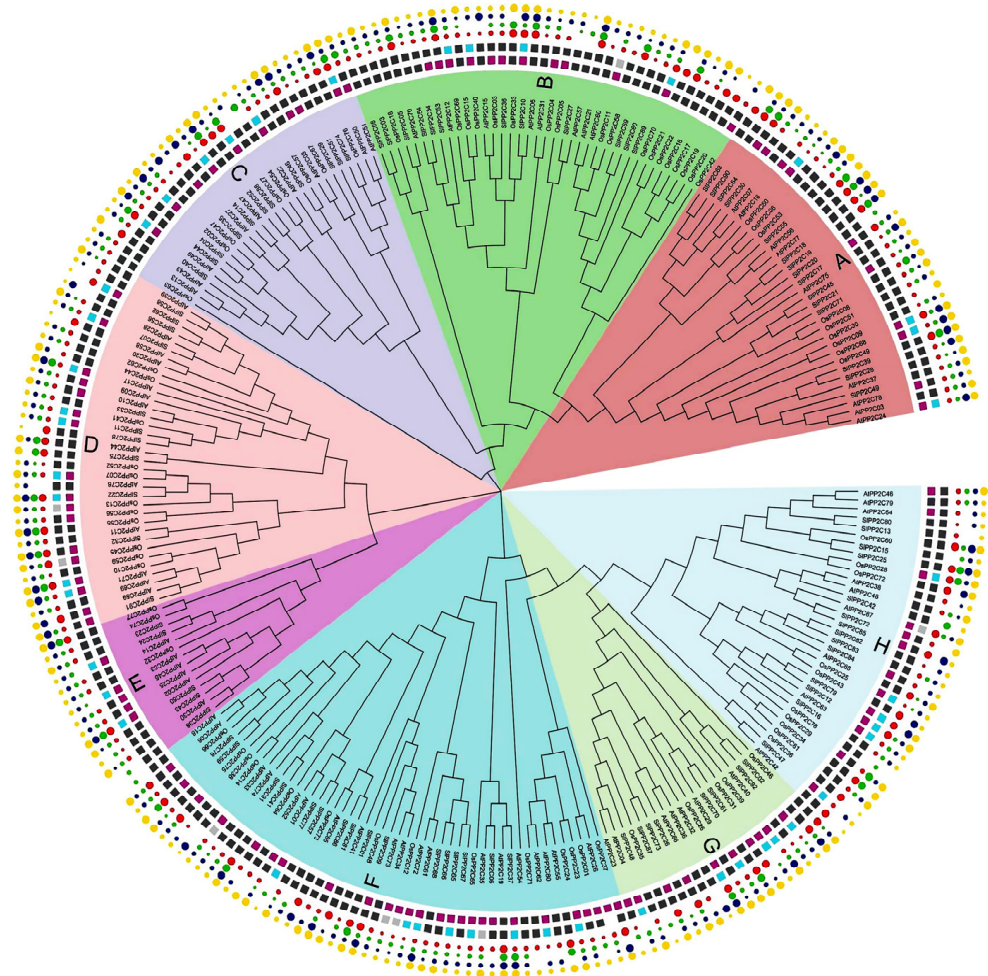


Figure 1. Phylogenetic analysis of the tomato *PP2C* family. It is based on protein sequence aligned by the ClustalW program. MEGA-X was used to construct a phylogenetic tree with the maximum likelihood method. Different colors indicate different subfamily members according to sequence similarity annotation analysis.

Duplication genes and their synonymous (K_s) and nonsynonymous (K_a) substitution rates (K_a/K_s) could reveal the evolutionary relationship and show the kind of selection pressure being encountered. K_a , K_s mutations, and K_a/K_s of 17 syntenic gene pairs of *SIPP2C* genes were calculated (Table 3, Supplementary Table S6). Commonly, if the value of $K_a/K_s < 1$, the duplicated gene pairs may evolve from purifying selection (also called negative selection); $K_a/K_s = 1$ means neutral selection; while $K_a/K_s > 1$ means positive selection [60]. The result proposed that 17 pairs of *SIPP2Cs* duplicated genes represented less than 1.00, suggesting that all duplicated *SIPP2C* genes have evolved mainly from purifying selection. We also calculated the divergence time (as $T = K_s/2\lambda$) among 17 pairs of duplicated *SIPP2C* genes based on a clock-like rate of 1.5×10^{-8} mutations per synonymous site per year, as proposed previously [61]. The result in Table 2 showed that divergence events of duplicated *SIPP2C* genes were estimated to have occurred around 2.33–73.33 Mya (million years ago). The average divergence time among these genes is 31.59 MYA.

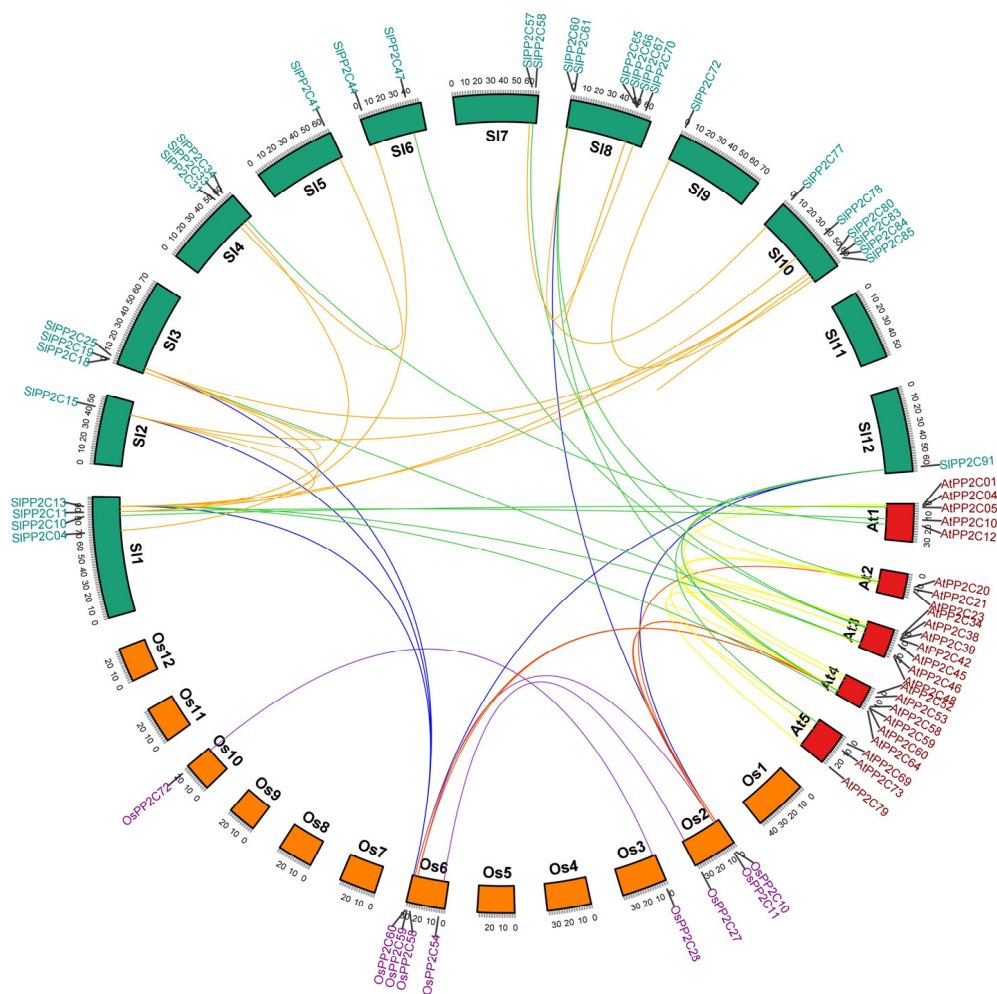


Figure 2. Duplication event analysis of *SIPP2C* genes and comparative synteny analysis among tomato, Arabidopsis, and rice, between tomato and Arabidopsis, and between tomato and rice. The red line represents the syntenic gene pairs between rice and Arabidopsis. The blue line indicates the syntenic gene pairs between rice and tomato. The green line represents the syntenic gene pairs between tomato and Arabidopsis. The golden line represents the syntenic gene pairs in tomato. The yellow line represents the syntenic gene pairs in Arabidopsis. The purple line represents the syntenic gene pairs in rice. Tomato chromosomes are depicted as green segments, and Arabidopsis and rice are shown in red and orange, respectively. The chromosome number and syntenic gene pairs are marked. The size of chromosomes was consistent with the actual pseudo-chromosome size. Positions are in Mb.

Table 3. *SIPP2C* syntenic gene pairs present in tomato genome.

Gene ID	Ka	Ks	Ka/Ks	Divergence Time (Myr)
<i>SIPP2C04/44</i>	0.09	0.69	0.12	23
<i>SIPP2C11/78</i>	0.1	0.54	0.19	18
<i>SIPP2C13/80</i>	0.08	0.63	0.12	21
<i>SIPP2C15/25</i>	0.07	0.6	0.11	20
<i>SIPP2C15/12</i>	0.12	2.04	0.06	68
<i>SIPP2C15/80</i>	0.14	2.2	0.06	73.33
<i>SIPP2C18/19</i>	0.08	0.09	0.93	3
<i>SIPP2C25/13</i>	0.14	2.01	0.07	67

Table 3. Cont.

Gene ID	Ka	Ks	Ka/Ks	Divergence Time (Myr)
<i>SIPP2C33/11</i>	0.19	1.68	0.11	56
<i>SIPP2C41/31</i>	0.28	0.85	0.33	28.33
<i>SIPP2C57/57</i>	0.09	0.75	0.12	25
<i>SIPP2C61/70</i>	0.09	0.72	0.12	24
<i>SIPP2C66/65</i>	0.08	0.37	0.22	12.33
<i>SIPP2C67/65</i>	0.02	0.07	0.26	2.33
<i>SIPP2C80/25</i>	0.15	1.93	0.08	64.33
<i>SIPP2C84/83</i>	0.08	0.12	0.64	4
<i>SIPP2C85/72</i>	0.12	0.82	0.15	27.33

3.3. Chromosomal Localization and Duplication of *SIPP2C* Genes

The 92 *SIPP2C* genes were mapped with the published chromosomes of the tomato genome to identify their distribution (Figure 3). They are scattered on 11 of the 12 chromosomes. Macroscopically, these *SIPP2Cs* were unevenly distributed across these chromosomes and mostly existed in the form of gene clusters. High-density regions harboring *PP2Cs* were found in chromosomes 01, 03, 06, 08, and 10 and discretely distributed in chromosomes 02, 04, 05, 07, 09, and 12. The most and the least *SIPP2Cs* were distributed on chromosome 03 (14 *SIPP2C* genes, accounting for 15.22%) and chromosome 02 (3 *SIPP2C* genes: 3.26%).

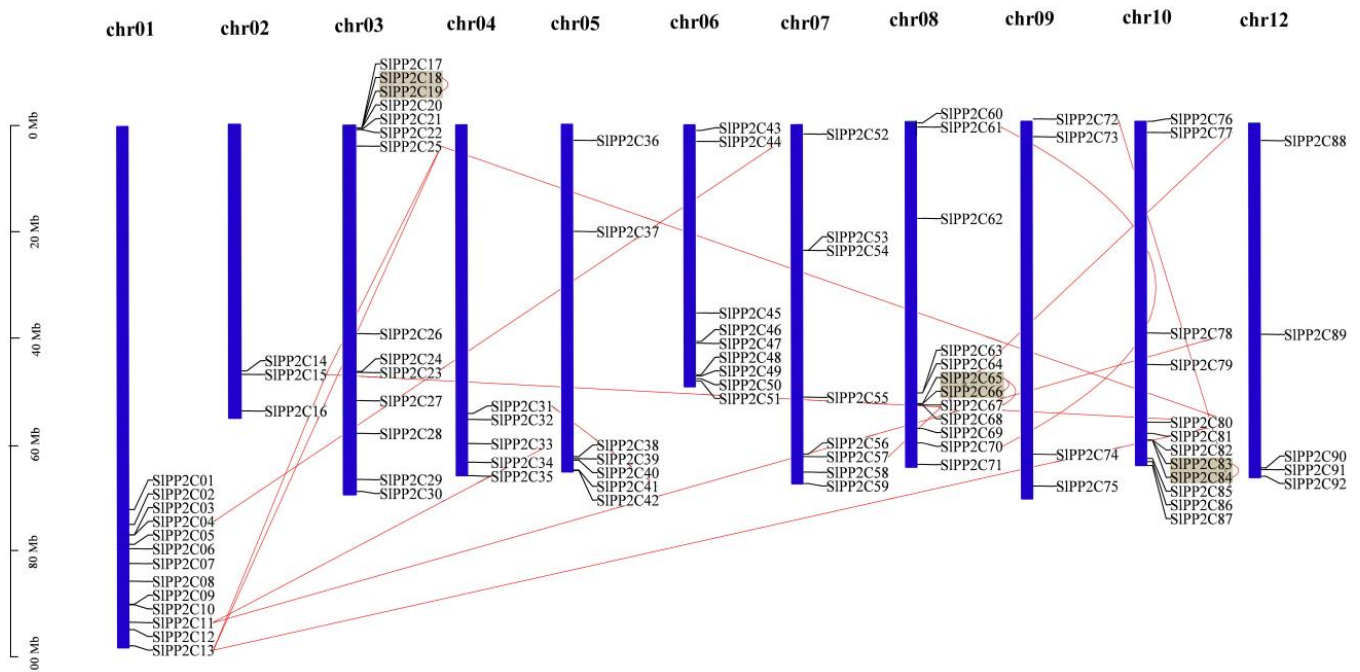


Figure 3. Chromosome distribution of tomato *PP2C* genes. Chromosome localization is based on the physical location (Mb) of 12 tomato chromosomes. Chromosome numbers are displayed at the top of each bar chart. Locations of tomato *PP2C* genes in chromosomes were obtained from the SGN (<http://solgenomics.net> (accessed on 5 March 2022)). Grey blocks were represented by the tandem duplicated genes, and the segmentally duplicated genes were linked by red lines. Scale bar on the left indicated the length (Mb) of tomato chromosomes.

Previous studies in rice, *Arabidopsis*, and *B. distachyon* showed that *PP2C* gene families mainly expanded by whole-genome and chromosomal segment duplication [14,33]. Closely related genes located within a distance of fewer than 200 kb on the same chromosome are defined as tandem duplications; otherwise, they are segmental duplication [62]. According to this principle, 17 pairs of duplication *SIPP2C* genes were found to be involved in segmental duplication events and three of them may be involved in tandem duplication. These 17 pairs of duplicated *SIPP2C* genes are distributed on chromosomes 01, 02, 03, 04, 05, 06, 07, 08, 09, and 10, but not on chromosome 12. These three pairs of tandem duplication are distributed on chromosomes 03, 08, and 10.

3.4. Conserved Motif and Gene Structure of *SIPP2Cs*

In order to better understand the conservation and diversity of motif compositions and gene structures of *SIPP2Cs*, the conserved motifs and exon–intron organization of *SIPP2Cs* were analyzed and a new phylogenetic tree as a reference was also structured (Figure 4). The conserved motifs of *SIPP2C* proteins were analyzed using the software MEME and 10 distinct conserved motifs were identified (Table 4). In Figure 4A, the number of motifs ranged from 1 to 10 with 15–50 residues in all *SIPP2C* proteins. Motifs 1, 2, 3, 4, 5, 6, 8, 9, and 10 ubiquitously existed in *SIPP2Cs*, which showed that these motifs may have similar conserved positions and functions. Interestingly, motif 7 was selectively presented in a few *SIPP2Cs*, and they all belong to group H. Therefore, motif 7 may have an unusually special role in the process of regulation.

Table 4. Conserved motifs in the amino acid sequences of *SIPP2C* proteins.

Motif	Width	Multilevel Consensus Sequence
 1	15	FLILASDGLWDVLSN
 2	21	VIQGETLYVANVGDSRAVLCR
 3	15	TFFGVYDGHGGPGAA
 4	20	VWRVKGGLAVSRAIGDKYLK
 5	15	AIQLSVDHKNREDE
 6	15	RGSHDBISVIVVFLD
 7	50	HEGGDLGGRQDGLLWYKDLGQHANGFEFSMAVVQANNLLEDQSQVESGPLS
 8	41	AVDIVHSYPRGGIARRLVKAAALQEAAKKREMRYSDLKKIDR
 9	20	SQQGRRGEMEDAHIVWPBFC
 10	14	KKALRKAFLKTDEE

The whole *SIPP2Cs* gene structures were analyzed using TBtools. As shown in Figure 4B, tomato *PP2C* gene exon–intron organizations were diverse. The difference in the number of exons (1–20) was apparent for *SIPP2Cs*. *SIPP2C74* was encoded by at least 20 exons which had the largest number of exons, whereas *SIPP2C51* only was encoded by one exon. Among the aligned 92 *SIPP2C* members, 98.91% of them had at least two introns except *SIPP2C51* where no introns were found. Furthermore, the members of the same group showed structural similarities, such as intron phase, intron number, and exon length. The result indicated that *SIPP2Cs* had evolutionary stability and versatility in tomato.

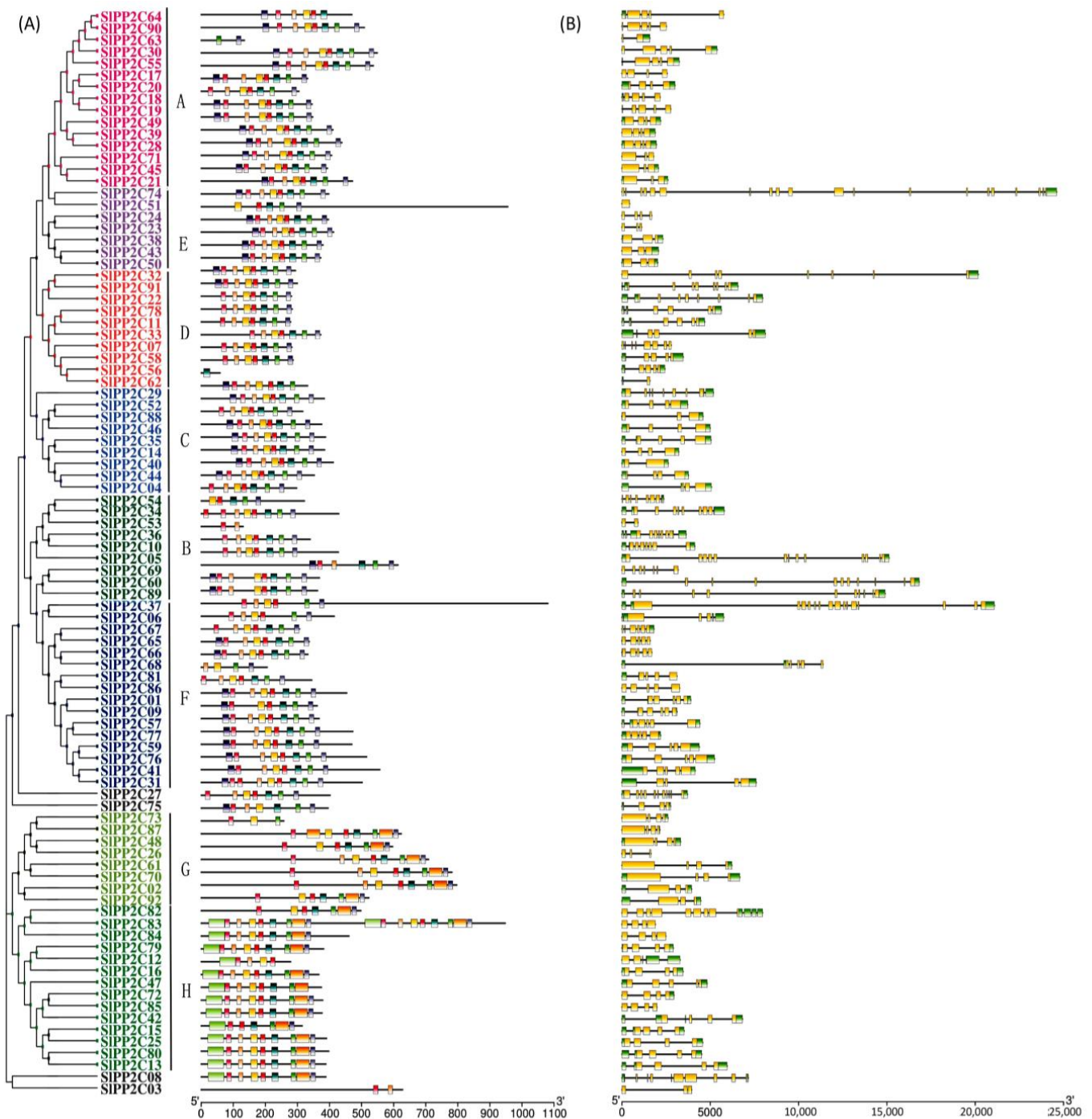


Figure 4. Phylogenetic relationships, conserved motifs of *SIPP2C* proteins, and structures of *SIPP2C* genes in tomato. (A) Arrangement of conserved motifs in *SIPP2C* proteins. Ten predicted motifs were represented by different colored boxes, and motif details referred to Table 3. A–H depicted that PP2C genes were divided into eight groups. Scale bar indicates amino acid length (B) Gene structure of *SIPP2C* members. The phylogenetic tree was constructed using MEGA-X software and the gene structures were visualized by TBtools. Boxes represented exons, and yellow boxes represented CDS and the upstream and downstream regions of *SIPP2C* genes were indicated by green boxes. For all genes, black lines represent introns. The sizes of genes can be estimated by the scale at the bottom.

3.5. Cis-Elements in the Promoters of Tomato PP2C Genes

Gene transcription levels were regulated by the interaction of transcription factors with the cis-acting element in the upstream promoter sequences. Therefore, studying the cis-element in the promoter of PP2C genes in the tomato may help decrypt the function of SIPP2C genes. The promoter regions (3 kb upstream ATG) of 92 SIPP2C genes were analyzed using the online software PlantCARE. After excluding the common cis-elements, such as the TATA-box and CAAT-box, the remaining 26 cis-elements can be divided into six parts (Table 5). Then depicted by TBtools (Figure 5, Supplementary Table S7). Eight cis-elements, namely, GT1-motif, G-box, MRE, ACE, 3-AF1 binding site, Sp1, 4cl-CMA2b, and AAAC-motif are associated with light responsiveness. Ten cis-elements, including CGTCA-motif, TGACG-motif, ABRE, TGA-, AuxRR-core, TCA-, SARE, GARE-motif, P-box, and TATC-box are related to hormone induction. Two stress-related elements, including MBS and LTR, are induced by abiotic and biotic stresses. O2-site and MBSI have a connection with growth and development. Moreover, an element called Box III, which is a protein binding site, a regulatory element called MSA-like, and an element circadian-related circadian is found. Clearly, many cis-elements related to abiotic stress in plants were identified at the promoter of PP2C gene, and the promoter of 70 out of 92 PP2C genes had ABRE (cis-element involved in the ABA responsiveness), indicating that PP2Cs played a decisive role in abiotic stress resistance via ABA response.

Table 5. Functionally annotated cis-elements identified in the promoters of 92 SIPP2Cs.

Cis-Element	Number of Genes	Functions of Cis-Elements
 circadian	19	circadian control
 GT1-motif	57	light responsiveness
 G-box	70	light responsiveness
 MRE	36	light responsiveness
 ACE	21	light responsiveness
 3-AF1	10	light responsive
 Sp1	9	light responsive
 4cl-CMA2b	1	light responsive
 AAAC-motif	3	light responsive
 CGTCA-motif	60	MeJA-responsiveness
 TGACG-motif	60	MeJA-responsiveness
 ABRE	70	abscisic acid responsiveness
 TGA-	26	auxin-responsive
 AuxRR-core	11	auxin responsiveness
 TCA-	47	salicylic acid responsiveness
 SARE	1	salicylic acid responsiveness
 GARE-motif	21	gibberellin-responsive
 P-box	31	gibberellin-responsive
 TATC-box	16	gibberellin-responsiveness
 LTR	24	low-temperature responsiveness
 MBS	38	drought-inducibility
 MBSI	8	flavonoid biosynthetic genes regulation
 MSA-like	4	cell cycle regulation
 O2-site	25	zein metabolism regulation
 Box III	4	protein binding site

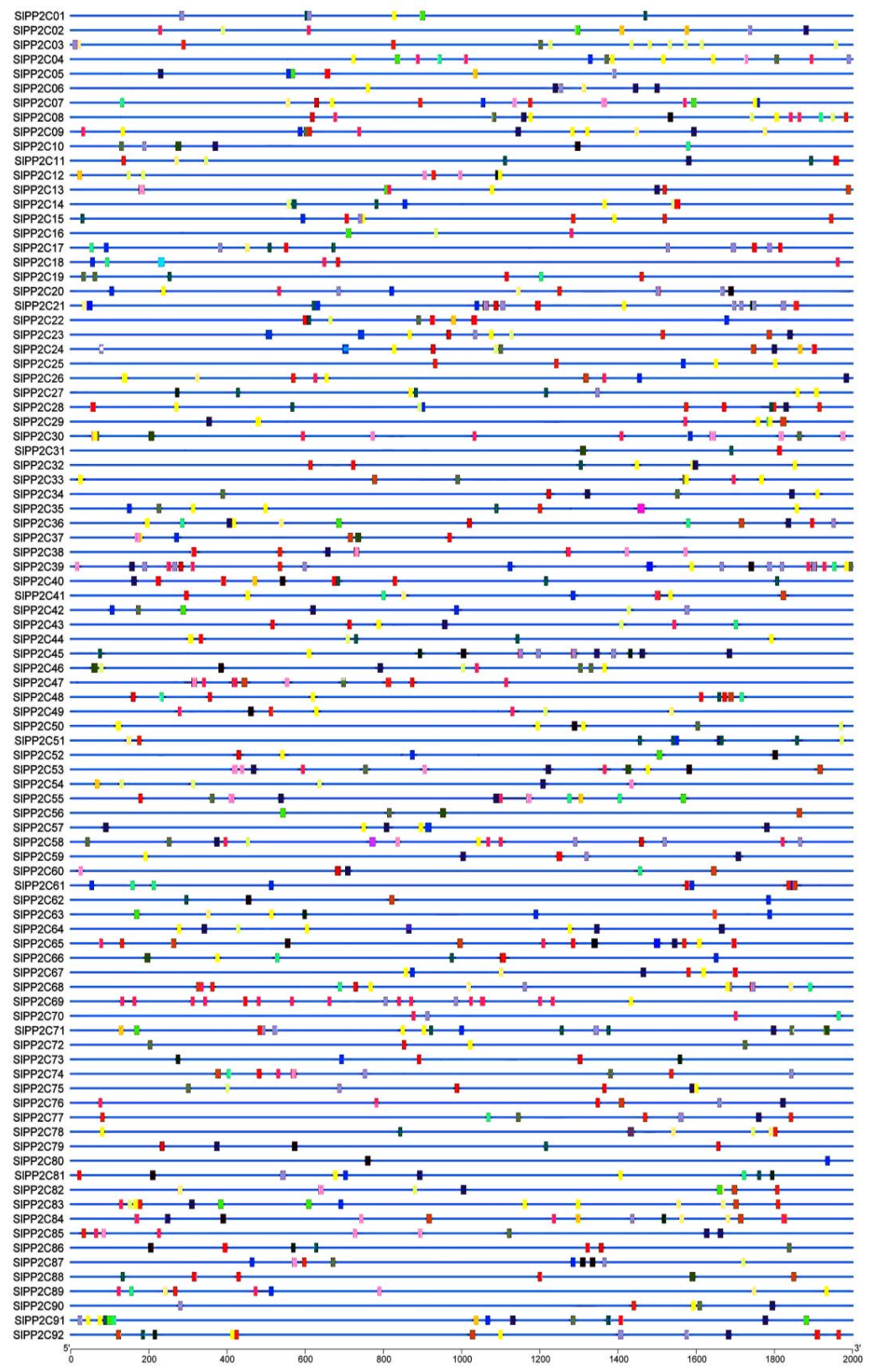


Figure 5. Identified cis-elements in the promoters of *SIPP2C* genes. The grey line represents the 2000 bp upstream of the *SIPPCs* transcription start site. Different colored wedges represent different cis-elements. The length and position of each *SIPP2C* gene are drawn to scale. Scale bar indicates DNA sequence length.

3.6. Expression of *SIPP2C* Genes in Different Tomato Tissues

The processes that *SIPP2C* genes may be involved in tomato growth and development were studied. The RNA-seq data of 10 tissues/stages, including roots, leaves, flowers, flower buds, 1, 2, and 3 cm fruits, mature green fruits, breaker fruits, and fruits on day 10 after breaking in Heinz were downloaded from TFGD to analyze the tissue expression pattern of *SIPP2Cs* (Supplementary Table S8). As shown in Figure 6, *SIPP2Cs* have different expression levels in different tissues and stages, 17 genes, including *SIPP2C04*, *SIPP2C10*, *SIPP2C11*, *SIPP2C13*, *SIPP2C22*, *SIPP2C30*, *SIPP2C31*, *SIPP2C32*, *SIPP2C39*, *SIPP2C55*, *SIPP2C58*, *SIPP2C60*, *SIPP2C78*, *SIPP2C79*, *SIPP2C80*, *SIPP2C90*, and *SIPP2C91* were highly expressed in all tissues/stages. By contrast, 14 genes, including *SIPP2C03*, *SIPP2C07*, *SIPP2C08*, *SIPP2C12*, *SIPP2C17*, *SIPP2C18*, *SIPP2C19*, *SIPP2C23*, *SIPP2C24*, *SIPP2C26*, *SIPP2C62*, *SIPP2C68*, *SIPP2C69*, and *SIPP2C71*, showed low expression levels in all tissues/stages. The expression patterns of the other *SIPP2Cs* showed different patterns of temporal and tissue-specific expressions. *SIPP2C67* was highly expressed in roots and *SIPP2C91* accumulated in the buds. *SIPP2C27* and *SIPP2C39* were expressed in leaves. In addition, four genes named *SIPP2C09*, *SIPP2C13*, *SIPP2C30*, and *SIPP2C91* were abundant in fully opened flowers. *SIPP2C58* was highly expressed in break fruit and +10 break fruit. Intriguingly, these genes indicated a possible role in the organ development of tomato.

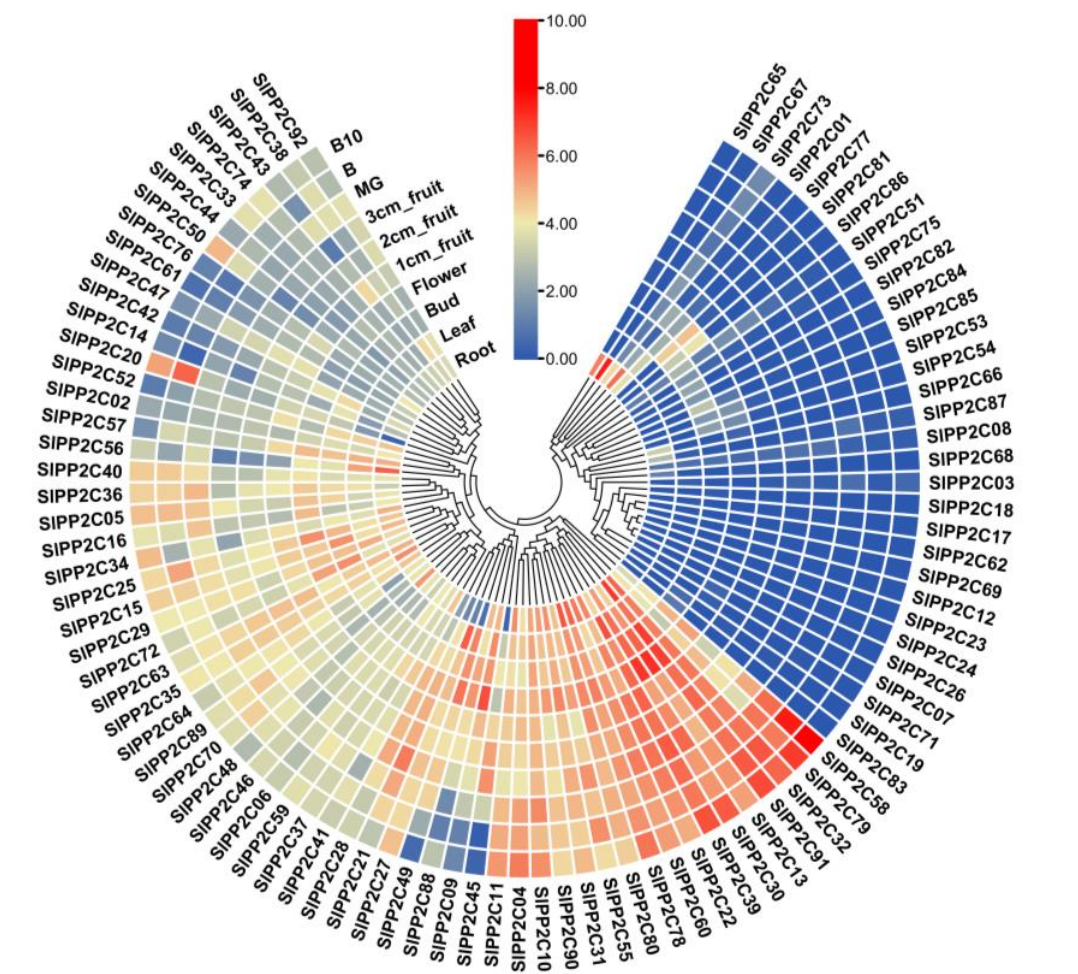


Figure 6. Heat map of the expression patterns of *SIPP2Cs* in 10 tissues/stages. Data of 10 tissues in the TFGD database were collected to reconstruct the expression pattern of *SIPP2C* genes. Heat map is presented in blue/yellow/red colors that indicate low/medium/high expression, respectively. The result was processed through cluster analysis.

3.7. Transcriptional Profiling of SIPP2C Genes of Tomato Infected with *Ralstonia solanacearum*

R. solanacearum, originally named *Pseudomonas solanacearum*, is a destructive soil-borne plant pathogen [63]. With strong environmental adaptability and a wide host range, it can cause lethal wilting diseases of 200 plant species [63], ranking second among the 10 most harmful plant pathogenic bacteria worldwide [64]. Many important economic crops in China such as peanut, potato, tomato, tobacco, and banana are deeply affected by this pathogen [63]. Therefore, we sequenced the stem of tomato infected with *R. solanacearum*. RNA-seq data were drawn into a heat map to further examine the expression patterns of SIPP2C genes under *R. solanacearum* infection treatment. In Figure 7, under *R. solanacearum*-infection condition, a total of 65 SIPP2C genes (70.65%) were found (Supplementary Table S9), nine SIPP2C genes (*SIPP2C28*, *SIPP2C38*, *SIPP2C40*, *SIPP2C43*, *SIPP2C44*, *SIPP2C48*, *SIPP2C50*, *SIPP2C89*, *SIPP2C92*) were obviously upregulated and three SIPP2C genes (*SIPP2C14*, *SIPP2C27*, and *SIPP2C36*) were obviously downregulated. This indicated that the function of SIPP2Cs might be related to *R. solanacearum* resistance.

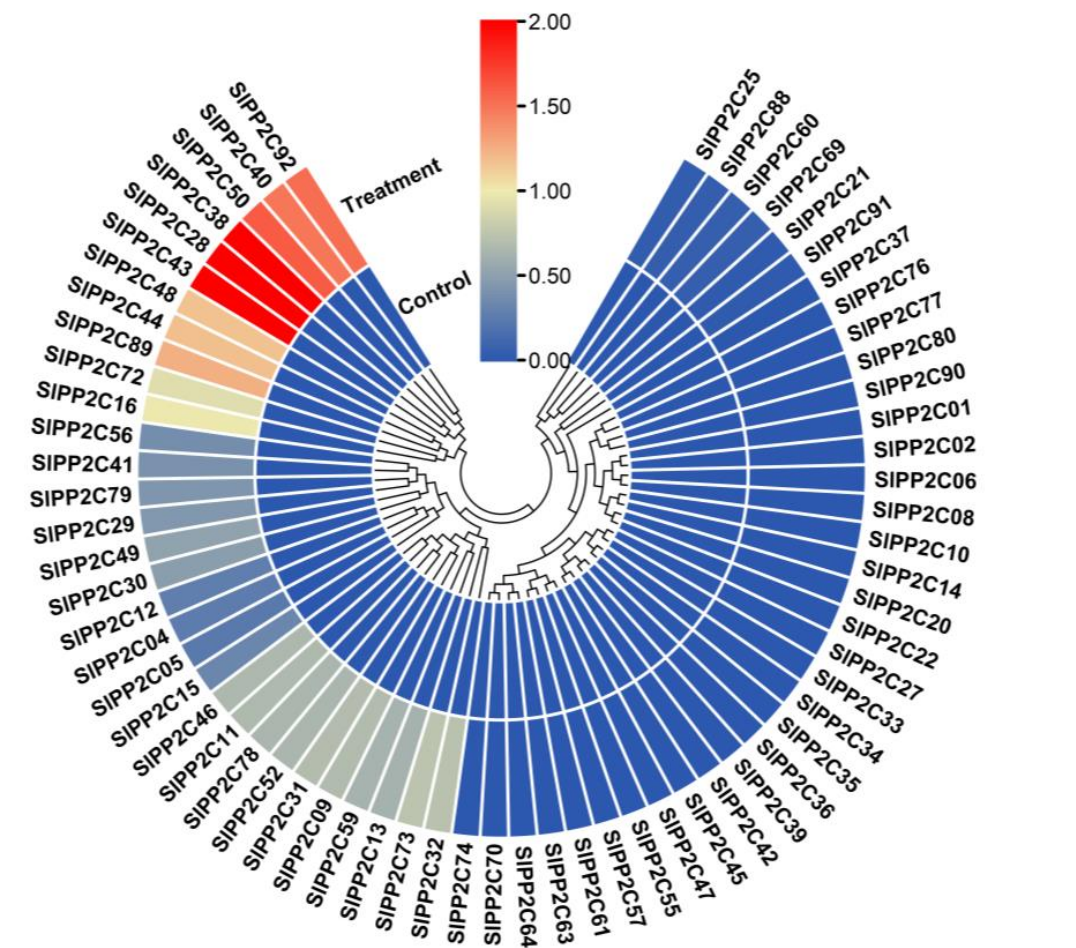


Figure 7. Expression profiles of SIPP2C genes in tomato roots infected by plant pathogen *Ralstonia solanacearum*. Blocks with colors represent decreased (blue) or increased (red) transcript levels relative to the control.

3.8. Analysis of SIPP2C Gene Expression in Tomato under *Ralstonia solanacearum* Infection

To further analyze the function of these gene families, qRT-PCR was used to investigate the expression of PP2C genes in tomato under *R. solanacearum* treatment. Based on the transcriptome data available in our laboratory, six upregulated and three downregulated expression genes were chosen. As shown in Figure 8, under *R. solanacearum* treatment, the expression levels of all five PP2C genes (*SIPP2C28*, *SIPP2C38*, *SIPP2C43*, *SIPP2C48*,

and *SIPP2C92*) have varying degrees of increasing, the expression of *SIPP2C40* change is not significant, but that of all three *PP2C* genes (*SIPP2C14*, *SIPP2C27*, and *SIPP2C36*) significantly decreased. This is mostly consistent with our transcriptome data. The small difference may be due to the inconsistency between the RNA-seq and qRT-PCR samples. The above transcriptome and qRT-PCR data indicated that the *PP2C* gene may play an important role in resistance to plant pathogen infection. Therefore, these genes are worthy of further functional verification experiments.

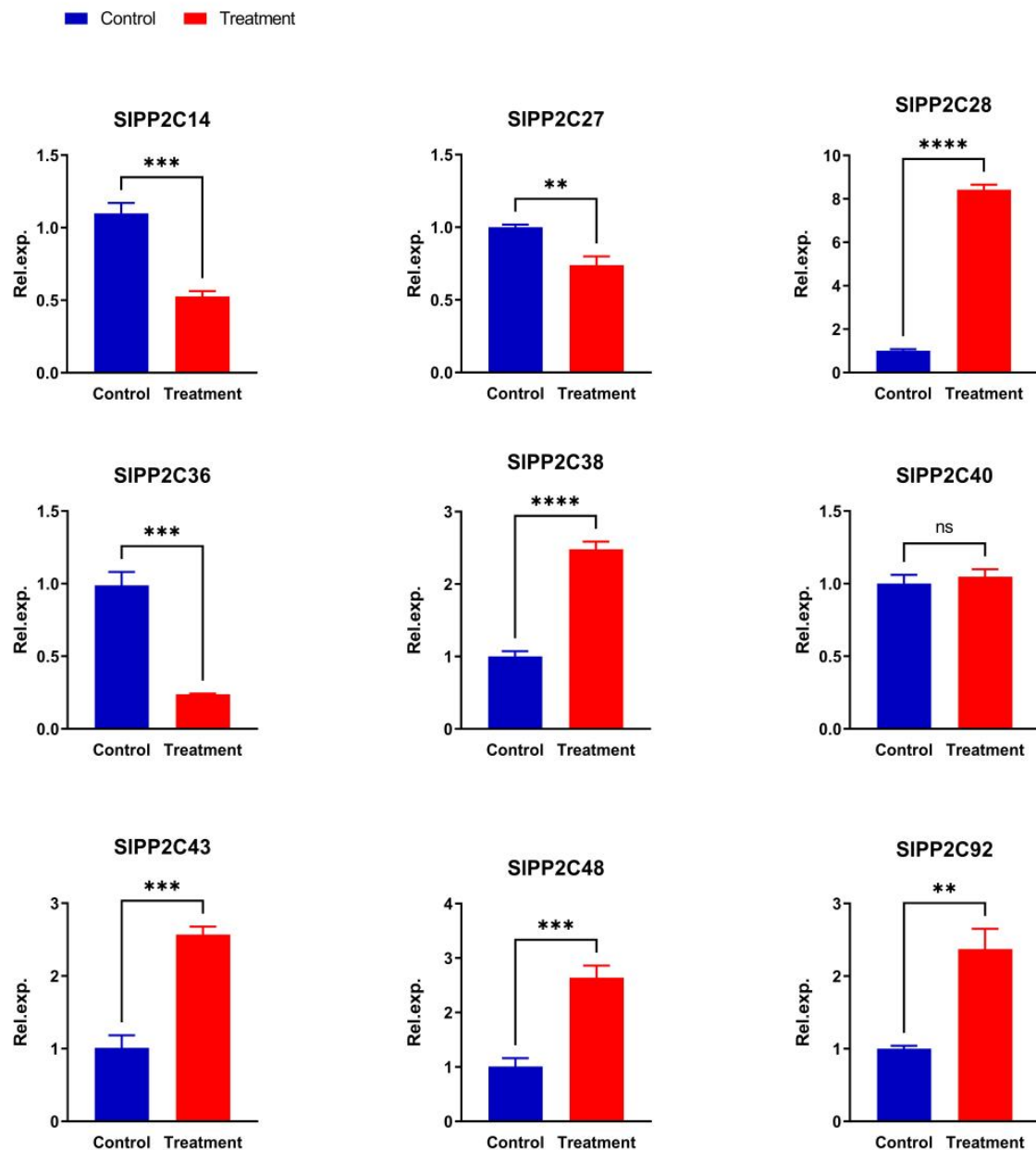


Figure 8. Expression of *SIPP2C* genes under plant pathogen *Ralstonia solanacearum* infection treatment. Control means untreated plants playing a controlling role. Treatment is *R. solanacearum* infection treatment plant. Expression of treated plants was compared with that in untreated plants after normalization of values with reference to the tomato β -actin gene and is presented as the relative expression level. All samples were collected from three biological replicates of each treatment at specified intervals. The error bars represent the SEM. ** $p < 0.01$, *** $p < 0.001$, **** $p < 0.0001$, Ns: not significant. The expression patterns of the selected *SIPP2C* genes were analyzed by qRT-PCR with gene-specific primers (Supplementary Table S8).

4. Discussion

The *PP2C* gene family is one of the most significant gene families that plays a vital role in response to stresses such as drought, salt, alkali, fungal pathogens as well as in plant development [65]. Previously, many studies have been carried out on the functional analysis of *PP2C* genes in Arabidopsis [66] and tobacco [67]. To date, many *PP2Cs* have already been identified in maize [7], rice [33], wheat [34], Arabidopsis [33], hot pepper [68], woodland strawberry [35], and *Medicago truncatula* [69] using advanced techniques of bioinformatics. In this study, a comprehensive genome-wide analysis of the *SIPP2Cs* gene family was performed, including gene identification, phylogenetic relationships, evolutionary analysis, synteny relationships, chromosomal localizations, gene structures, conserved domains, and motifs. In addition, gene expression patterns of some key *SIPP2C* genes were also determined under pathogen stress conditions. Herein, a total of 92 *SIPP2C* genes were identified.

4.1. Evolution of the *SIPP2C* Gene Family

PP2Cs have been evolutionarily conserved from prokaryotes to higher eukaryotes. Compared to other gene families, the *PP2C* gene family is one of the largest families in the plant kingdom. In lower plants, such as *Chlamydomonas reinhardtii*, *Physcomitrella patens*, and *Selaginella tamariscina*, the *PP2C* gene family members are much less common than those in higher plants. The increase in the diversity and the total number of *PP2C* genes from lower plants to higher plants may correlate with adaptations to the environmental stresses [70].

Gene duplication is one of the main driving forces of biological evolution [71], and it may contribute to the diversity of *SIPP2C*. The prediction of evolutionary patterns by calculating *Ka/Ks* provides information about the type of selection, such as purifying, positive, and neutral selection of gene pairs during divergence [72]. In this study, 17 *SIPP2C* tandem repeat gene pairs were identified. *Ka/Ks* of these tandem repeats were calculated. The result showed that *Ka/Ks* for 17 pairs of duplicated *SIPP2C* genes was <1 , suggesting that all duplicated *SIPP2C* genes have evolved mainly from purifying selection. This conclusion was mutually corroborated with the fact that the members of the *SIPP2C* gene family were conserved. In evolution, most of the genes copied from *SIPP2Cs* are adjacent to parental genes. Furthermore, for divergence time, we further utilized *Ks* values. The divergence time ranged from 0.07 to 2.2 (*Ks* values) and the mean duplication time is 31.59 MYA of these paralogous genes, which suggested that their divergence occurred later than the divergence time of Arabidopsis (about 16.1 MYA) [35]. The findings of our study demonstrated that Arabidopsis *AtPP2Cs* duplication time is much earlier than that of tomato *SIPP2C*. Therefore, the functional study of *AtPP2Cs* in Arabidopsis can provide a research basis for the study of *SIPP2C*.

4.2. Expression of *SIPP2Cs*

Environmental conditions cannot always maintain the optimal state needed for plant growth without artificial control. Therefore, plants are constantly challenged by a variety of environmental abiotic stress factors, such as drought, salt, high/low temperature, and biological stresses. These stresses seriously affect the yield and quality of tomato [73,74]. Until now, molecular mechanisms of plant responses to the above stress have been extensively studied. Plant hormones, such as ABA, SA, and GA, play a vital role in the ability of plants to cope with abiotic stresses by mediating growth, development, nutrient allocation, and source/sink transitions [75]. Among these, the significance of ABA signaling is well-documented in stress-adaptive modifications and stress resistance mechanisms. All *PP2C* group A genes in rice could be induced by ABA, and their relative expression levels were increased under high salt and low temperature treatment [33]. In Arabidopsis *ABI1*, *ABI2*, *HAB1*, *HAB2*, *AHG1*, and *PP2C-A* have reported encoding in ABA signaling networks [76–80]. Previous studies reported that *PP2C* regulates positively against salt tolerance in Arabidopsis and drought in peach to modulate the stress severity [81,82]. For

example, the Arabidopsis *AtPP2CG1* positively modulates the abiotic stresses, including salt, drought, and ABA [81]. The *ZmPP2C-A10* gene has a negative regulatory role in maize response to drought stress [23]. Moreover, not all *PP2C* genes have a similar response to abiotic stresses. In Arabidopsis, two members of *PP2C* genes responded differently, such as *AP2C1* expression was strongly induced by cold, drought, and wounding, but *AP2C2* was slightly influenced under the same treatments, suggesting their functional diversity [83]. Arabidopsis *PP2C-D* is mainly expressed in the roots, while the wild soybean *PP2C-D* is mainly expressed in the stem. Therefore, the wild soybean *PP2C-D* and Arabidopsis *PP2C-D* have different regulatory roles in different stress. Some *PP2C-D* in wild and cultivated soybean are involved in different signal transduction pathways; thus, adapting to different resistance mechanisms [84]. These findings highlighted the significance of the *PP2C* gene family. Aiming to obtain gene expression patterns of *SIPP2C*, we downloaded the previously reported RNA-sequence data and analyzed the expression profile of *PP2C* genes. By comparing *PP2C* gene transcription profiling in 10 tissues/stages, including leaves, roots, flowers, flower buds, 1, 2, and 3 cm fruits, mature green fruits, breaker fruits, and fruits on day 10 after breaking, the expression of all the *SIPP2C* genes showed diverse tissue-specific patterns, such as some of the genes were highly expressed in all the tissues, while some expressed only in one and/or two tissues, intimating that *SIPP2C* proteins may play multiple roles in plants. Thus, their functions are worthy of further study.

The yield of crops is largely affected by different types of biotic stresses [85]. Many abiotic stress conditions have been shown to weaken the defense mechanism of plants and enhance their sensitivity to pathogen infection [86,87]. Thus, finding resistance genes that can resist pathogen infection is very important to improve crop yield. Previous studies have shown that *PP2C* proteins play multiple roles in plants. In the case of tomato infected with *R. solanacearum*, RNA-seq and expression pattern of some *SIPP2Cs* were explored. *R. solanacearum* is a devastating soil-borne plant pathogen that brings serious losses to tomato production [63]. In our study, nine *SIPP2C* genes were upregulated under *R. solanacearum* infection treatment, showing that the *SIPP2C* gene family was indeed closely related to *R. solanacearum*. However, understanding whether or not each gene plays a critical role in abiotic stress tolerance still requires functional characterization of individual genes.

4.3. Possible Function of *SIPP2Cs*

The combination of our research and previous studies revealed that *SIPP2Cs* might have a variety of functions. The subcellular localization indicated that *SIPP2Cs* mainly had enzyme catalytic function in the cytoplasm and a few of them appeared in other cellular compartments, which may take part in other biochemical processes. For example, *AtAPD7*, an Arabidopsis *PP2C* protein, widely acted in the nucleus and cytoplasm of root cells and cytoplasm of mesophyll protoplasts [88]. *OsSIPP2C1* was located in the nucleus and it was negatively regulated by *ABL1* which could respond to abiotic stresses and regulate panicle development in rice [89]. The cis-element analysis revealed that there were many light response elements in the promoter regions of *SIPP2C* genes, such as sp1, G-box, ACE, and 3-AF1 binding sites. Among them, G-box appeared in 70 out of 92 *SIPP2Cs*, which may have an important influence on regulating tomato accumulation dry matter by light and action. Furthermore, a large number of stress- and hormone-related elements were also found, such as ABA-responsive elements (ABREs) that are responsive to ABA, drought, or salt signals [90], LTR is involved in low-temperature response and regulation [91], TCA-element and CGTCA-motif have good correlation with the expression levels after MeJA and SA treatment [92], respectively. Further elucidating the predicated and the possible functions of *SIPP2C* genes in transcriptional regulation, the result represented significant variation among *SIPP2C* genes and was mostly responsive to *R. solanacearum*. Therefore, *PP2C* genes play a very important role in abiotic stress or biotic stress. It is of great research significance.

5. Conclusions

In this study, the *PP2C* gene family in tomato was classified and general analysis of the 92 members in this family was carried out including the proteins' physical and chemical properties, subcellular localization, evolutionary relationship, gene duplication, environmental pressure, gene structure, conserved domains, cis-acting elements, conserved motifs, and expression patterns. Most of them showed tissue and developmental stage-specific expression profiles, and some of them can be induced by biotic stress (*R. solanacearum*), indicating that the *SIPP2Cs* play an important role in plants. The results of this study laid a foundation for more in-depth genetic transformation and gene function analysis and were necessary to advance research on the stress resistance of tomato. In summary, the integration of our findings has provided a novel insight and unique features of *SIPP2C* genes, which is also important for accelerating the cloning of stress resistance genes in tomato.

Supplementary Materials: The following supporting information can be downloaded at: <https://www.mdpi.com/article/10.3390/genes13040604/s1>, Supplementary Table S1: List of primers used for RT-PCR; Supplementary Table S2: The *PP2C* genes ID were submitted into SGN; Supplementary Table S3: The *PP2C* gene family of Arabidopsis and rice; Supplementary Table S4: Total number of *PP2C* genes participating in the synteny relationship; Supplementary Table S5: The syntenic *PP2C* gene pairs in tomato, Arabidopsis, rice, and between them; Supplementary Table S6: KaKs of all *SIPP2Cs* tandem repeat gene pairs; Supplementary Table S7: Cis-elements identified in the promoters of *SIPP2Cs*; Supplementary Table S8: Expression of *PP2C* genes in different Henzi tomato tissues; Supplementary Table S9: Information of probe sets used for microarray expression analysis.

Author Contributions: The work presented here was carried out in collaboration between all authors. Conceptualization, J.Q., L.N. and X.Z.; methodology, X.Z.; software, J.Q., L.N. and X.X.; validation, J.Q.; formal analysis, J.Q. and L.N.; investigation, J.Q.; resources, J.Q. and L.N.; data curation, X.X., S.C., Y.Z., M.L. (Min Lang), M.L. (Mengyu Li) and B.L.; writing—original draft preparation, J.Q. and L.N.; writing—review and editing, J.Q., L.N. and X.Z.; visualization, J.Q.; supervision, X.Z., J.L. and Y.P.; project administration, X.Z.; funding acquisition, X.Z. All authors have read and agreed to the published version of the manuscript.

Funding: This research was funded by the National Natural Science Foundation of China grant number (#31872119).

Data Availability Statement: Not applicable.

Conflicts of Interest: The authors declare no conflict of interest.

References

1. Long, L.; Gao, W.; Xu, L. GbMPK3, a mitogen-activated protein kinase from cotton, enhances drought and oxidative stress tolerance in tobacco. *Plant Cell Tissue Organ Cult.* **2014**, *116*, 153–162. [[CrossRef](#)]
2. Sheng, L. Protein phosphatases and signaling cascades in higher plants. *Trends Plant Sci.* **1998**, *3*, 271–275.
3. Mizoguchi, T.; Ichimura, K.; Shinozaki, K. Environmental stress response in plants: The role of mitogen-activated protein kinases. *Trends Biotechnol.* **1997**, *15*, 15–19. [[CrossRef](#)]
4. Boudsocq, M.; Barbier-Brygoo, H.; Lauriere, C. Identification of nine sucrose nonfermenting 1-related protein kinases 2 activated by hyperosmotic and saline stresses in *Arabidopsis thaliana*. *J. Biol. Chem.* **2004**, *279*, 41758–41766. [[CrossRef](#)]
5. Ma, S.Y.; Wu, W.H. AtCPK23 functions in *Arabidopsis* responses to drought and salt stresses. *Plant Mol. Biol.* **2007**, *65*, 511–518. [[CrossRef](#)]
6. Franz, S.; Ehlert, B.; Liese, A.; Kurth, J.; Cazalé, A.C.; Romeis, T. Calcium-dependent protein kinase CPK21 functions in abiotic stress response in *Arabidopsis thaliana*. *Mol. Plant* **2011**, *4*, 83–96. [[CrossRef](#)]
7. Wei, K.; Pan, S. Maize protein phosphatase gene family: Identification and molecular characterization. *BMC Genom.* **2014**, *15*, 773. [[CrossRef](#)]
8. Kerk, D.; Templeton, G.; Moorhead, G.B. Evolutionary radiation pattern of novel protein phosphatases revealed by analysis of protein data from the completely sequenced genomes of humans, green algae, and higher plants. *Plant Physiol.* **2008**, *146*, 351–367. [[CrossRef](#)]
9. Cohen, P. The structure and regulation of protein phosphatases. *Annu. Rev. Biochem.* **1989**, *58*, 453–508. [[CrossRef](#)]
10. Singh, A.; Pandey, A.; Srivastava, A.K.; Tran, L.S.; Pandey, G.K. Plant protein phosphatases 2C: From genomic diversity to functional multiplicity and importance in stress management. *Crit. Rev. Biotechnol.* **2016**, *36*, 1023–1035. [[CrossRef](#)]

11. Chae, L.; Pandey, G.K.; Luan, S.; Cheong, Y.H.; Kim, K. Protein kinases and phosphatases for stress signal transduction in plants. In *Abiotic Stress Adaptation in Plants*; Springer: Berlin/Heidelberg, Germany, 2010; pp. 123–163.
12. Mackintosh, C.; Coggins, J.; Cohen, P. Plant protein phosphatases. subcellular distribution, detection of protein phosphatase 2C and identification of protein phosphatase 2A as the major quinate dehydrogenase phosphatase. *Biochem. J.* **1991**, *273*, 733–738. [[CrossRef](#)]
13. Schweighofer, A.; Hirt, H.; Meskiene, I. Plant PP2C phosphatases: Emerging functions in stress signaling. *Trends Plant Sci.* **2004**, *9*, 236–243. [[CrossRef](#)]
14. Cao, J.; Jiang, M.; Li, P.; Chu, Z. Genome-wide identification and evolutionary analyses of the PP2C gene family with their expression profiling in response to multiple stresses in *Brachypodium distachyon*. *BMC Genom.* **2016**, *17*, 175. [[CrossRef](#)]
15. Singh, A.; Giri, J.; Kapoor, S.; Tyagi, A.K.; Pandey, G.K. Protein phosphatase complement in rice: Genome-wide identification and transcriptional analysis under abiotic stress conditions and reproductive development. *BMC Genom.* **2010**, *11*, 435. [[CrossRef](#)]
16. Sugimoto, H.; Kondo, S.; Tanaka, T.; Imamura, C.; Muramoto, N.; Hattori, E.; Ogawa, K.; Mitsukawa, N.; Ohto, C. Overexpression of a novel *Arabidopsis* PP2C isoform, AtPP2CF1, enhances plant biomass production by increasing inflorescence stem growth. *J. Exp. Bot.* **2014**, *65*, 5385–5400. [[CrossRef](#)]
17. Manohar, M.; Wang, D.; Manosalva, P.M.; Choi, H.W.; Kombrink, E.; Klessig, D.F. Members of the abscisic acid co-receptor PP2C protein family mediate salicylic acid–abscisic acid crosstalk. *Plant Direct* **2017**, *1*, e00020. [[CrossRef](#)]
18. Komatsu, K.; Suzuki, N.; Kuwamura, M.; Nishikawa, Y.; Nakatani, M.; Ohtawa, H.; Takezawa, D.; Seki, M.; Tanaka, M.; Taji, T.; et al. Group A PP2Cs evolved in land plants as key regulators of intrinsic desiccation tolerance. *Nat. Commun.* **2013**, *4*, 2219. [[CrossRef](#)]
19. Rodriguez, P.L.; Leube, M.P.; Grill, E. Molecular cloning in *Arabidopsis thaliana* of a new protein phosphatase 2C (PP2C) with homology to ABI1 and ABI2. *Plant Mol. Biol.* **1998**, *38*, 879–883. [[CrossRef](#)]
20. Gosti, F.; Beaudoin, N.; Serizet, C.; Webb, A.A.; Vartanian, N.; Giraudat, J. ABI1 protein phosphatase 2C is a negative regulator of abscisic acid signaling. *Plant Cell* **1999**, *11*, 1897–1910. [[CrossRef](#)]
21. Merlot, S.; Gosti, F.; Guerrier, D.; Vavasseur, A.; Giraudat, J. The ABI1 and ABI2 protein phosphatases 2C act in a negative feedback regulatory loop of the abscisic acid signalling pathway. *Plant J.* **2010**, *25*, 295–303. [[CrossRef](#)]
22. Zhang, Y.; Li, Q.; Jiang, L.; Kai, W.; Liang, B.; Wang, J.; Du, Y.; Zhai, X.; Wang, J.; Zhang, Y.; et al. Suppressing type 2C protein phosphatases alters fruit ripening and the stress response in tomato. *Plant Cell Physiol.* **2018**, *59*, 142–154. [[CrossRef](#)]
23. Xiang, Y.; Sun, X.; Gao, S.; Qin, F.; Dai, M. Deletion of an endoplasmic reticulum stress response element in a *ZmPP2C-A* gene facilitates drought tolerance of maize seedlings. *Mol. Plant* **2017**, *10*, 456–469. [[CrossRef](#)]
24. Arshad, M.; Mattsson, J. A putative poplar PP2C-encoding gene negatively regulates drought and abscisic acid responses in transgenic *Arabidopsis thaliana*. *Trees* **2014**, *28*, 531–543. [[CrossRef](#)]
25. Wang, Y.; Chen, P.; Sun, L.; Li, Q.; Dai, S.; Sun, Y. Transcriptional regulation of *PaPYLs*, *PaPP2Cs* and *PaSnRK2s* during sweet cherry fruit development and in response to abscisic acid and auxin at onset of fruit ripening. *Plant Growth Regul.* **2015**, *75*, 455–464. [[CrossRef](#)]
26. Zhang, F.; Wei, Q.; Shi, J.; Jin, X.; He, Y.; Zhang, Y.; Luo, Q.; Wang, Y.; Chang, J.; Yang, G.; et al. *Brachypodium distachyon* BdPP2CA6 interacts with BdPYLs and BdSnRK2 and positively regulates salt tolerance in transgenic *Arabidopsis*. *Front. Plant Sci.* **2017**, *8*, 264. [[CrossRef](#)]
27. Schweighofer, A.; Kazanaviciute, V.; Scheikl, E.; Teige, M.; Doczi, R.; Hirt, H.; Schwanninger, M.; Kant, M.; Schuurink, R.; Mauch, F.; et al. The PP2C-type phosphatase AP2C1, which negatively regulates MPK4 and MPK6, modulates innate immunity, jasmonic acid, and ethylene levels in *Arabidopsis*. *Plant Cell* **2007**, *19*, 2213–2224. [[CrossRef](#)]
28. Shubchynskyy, V.; Boniecka, J.; Schweighofer, A.; Simulis, J.; Kvederaviciute, K.; Stumpe, M.; Mauch, F.; Balazadeh, S.; Mueller-Roeber, B.; Boutrot, F.; et al. Protein phosphatase AP2C1 negatively regulates basal resistance and defense responses to *Pseudomonas syringae*. *J. Exp. Bot.* **2017**, *68*, 1169–1183.
29. Sidonskaya, E.; Schweighofer, A.; Shubchynskyy, V.; Kammerhofer, N.; Hofmann, J.; Wiczorek, K.; Meskiene, I. Plant resistance against the parasitic nematode *Heterodera schachtii* is mediated by MPK3 and MPK6 kinases, which are controlled by the MAPK phosphatase AP2C1 in *Arabidopsis*. *J. Exp. Bot.* **2016**, *67*, 107–118. [[CrossRef](#)]
30. Umbrasaitte, J.; Schweighofer, A.; Kazanaviciute, V.; Magyar, Z.; Ayatollahi, Z.; Unterwurzacher, V.; Choopayak, C.; Boniecka, J.; Murray, J.A.; Bogre, L.; et al. MAPK phosphatase AP2C3 induces ectopic proliferation of epidermal cells leading to stomata development in *Arabidopsis*. *PLoS ONE* **2010**, *5*, 15357. [[CrossRef](#)]
31. Tovar-Mendez, A.; Miernyk, J.A.; Hoyos, E.; Randall, D.D. A functional genomic analysis of *Arabidopsis thaliana* PP2C clade D. *Protoplasma* **2014**, *251*, 265–271. [[CrossRef](#)]
32. Min, W.L.; Jelenska, J.; Greenberg, J.T. *Arabidopsis* proteins important for modulating defense responses to *Pseudomonas syringae* that secrete HopW1-1. *Plant J.* **2010**, *54*, 452–465.
33. Xue, T.; Wang, D.; Zhang, S. Genome-wide and expression analysis of protein phosphatase 2C in rice and *Arabidopsis*. *BMC Genom.* **2008**, *9*, 550. [[CrossRef](#)] [[PubMed](#)]
34. Yu, X.; Han, J.; Wang, E.; Xiao, J.; Hu, R.; Yang, G.; He, G. Genome-wide identification and homoeologous expression analysis of PP2C genes in wheat (*Triticum aestivum* L.). *Front. Genet.* **2019**, *10*, 561. [[CrossRef](#)] [[PubMed](#)]

35. Haider, M.S.; Khan, N.; Pervaiz, T.; Zhongjie, L.; Nasim, M.; Jogaiah, S.; Mushtaq, N.; Jiu, S.; Jinggui, F. Genome-wide identification, evolution, and molecular characterization of the PP2C gene family in woodland strawberry. *Gene* **2019**, *702*, 27–35. [[CrossRef](#)]
36. Khan, N.; Ke, H.; Hu, C.M.; Naseri, E.; Haider, M.S.; Ayaz, A.; Amjad, K.W.; Wang, J.; Hou, X. Genome-wide identification, evolution, and transcriptional profiling of PP2C gene family in *Brassica rapa*. *BioMed Res. Int.* **2019**, *2019*, 2965035. [[CrossRef](#)]
37. Hosmani, P.S.; Flores-Gonzalez, M.; van de Geest, H.; Maumus, F.; Bakker, L.V.; Schijlen, E.; van Haarst, J.; Cordewener, J.; Sanchez-Perez, G.; Peters, S.; et al. An improved de novo assembly and annotation of the tomato reference genome using single-molecule sequencing, Hi-C proximity ligation and optical maps. *bioRxiv* **2019**, 767764. [[CrossRef](#)]
38. Wang, Y.F.; Liao, Y.Q.; Wang, Y.P. Genome-wide identification and expression analysis of StPP2C gene family in response to multiple stresses in potato (*Solanum tuberosum* L.). *J. Integr. Agric.* **2020**, *19*, 1609–1624. [[CrossRef](#)]
39. Jaina, M.; Sara, C.; Lowri, W. Pfam: The protein families database in 2021. *Nucleic Acids Res.* **2021**, *49*, 412–419.
40. Potter, S.C.; Luciani, A.; Eddy, S.R.; Park, Y.; Lopez, R.; Finn, R.D. HMMER web server: 2018 update. *Nucleic Acids Res.* **2018**, *1*, 200–204. [[CrossRef](#)]
41. Fernandez-Pozo, N.; Menda, N.; Edwards, J.D.; Saha, S.; Tecle, I.Y.; Strickler, S.R.; Bombarely, A.; Fisher-York, T.; Pujar, A.; Foerster, H.; et al. The Sol Genomics Network (SGN)—From genotype to phenotype to breeding. *Nucleic Acids Res.* **2015**, *43*, 1036–1041. [[CrossRef](#)]
42. Letunic, I.; Khedkar, S.; Borkm, P. SMART: Recent updates, new developments and status in 2020. *Nucleic Acids Res.* **2021**, *49*, 458–460. [[CrossRef](#)]
43. Lu, S.; Wang, J.; Chitsaz, F.; Derbyshire, M.K.; Geer, R.C.; Gonzales, N.R.; Gwadz, M.; Hurwitz, D.I.; Marchler, G.H.; Song, J.S.; et al. CDD/SPARCLE: The conserved domain database in 2020. *Nucleic Acids Res.* **2019**, *48*, 265–268. [[CrossRef](#)]
44. Duvaud, S.; Gabella, C.; Lisacek, F.; Stockinger, H.; Ioannidis, V.; Durinx, C. ExPasy, the swiss bioinformatics resource portal, as designed by its users. *Nucleic Acids Res.* **2021**, *49*, 216–227. [[CrossRef](#)]
45. Chou, K.C.; Shen, H.B. Plant-mPLoc: A top-down strategy to augment the power for predicting plant protein subcellular localization. *PLoS ONE* **2010**, *5*, e11335. [[CrossRef](#)]
46. Hung, J.H.; Weng, Z. Sequence alignment and homology search with BLAST and ClustalW. *Cold Spring Harb. Protoc.* **2016**, *11*, pdb-rot093088.
47. Kumar, S.; Stecher, G.; Li, M.; Niyaz, C.; Tamura, K. MEGA X: Molecular Evolutionary genetics analysis across computing platforms. *Mol. Biol. Evol.* **2018**, *6*, 1547–1549. [[CrossRef](#)]
48. Gu, Z.; Cavalcanti, A.; Chen, F.C.; Bouman, P.; Li, W.H. Extent of gene duplication in the genomes of drosophila, nematode, and yeast. *Mol. Biol. Evol.* **2002**, *3*, 256–262. [[CrossRef](#)]
49. Zhang, Z. KaKs_calculator 3.0: Calculating selective pressure on coding and non-coding sequences. *Genom. Proteom. Bioinform.* **2022**. [[CrossRef](#)]
50. Chen, C.; Chen, H.; Zhang, Y.; Thomas, H.R.; Frank, M.H.; He, Y.; Xia, R. TBtools: An integrative toolkit developed for interactive analyses of big biological data. *Mol. Plant* **2020**, *13*, 1194–1202. [[CrossRef](#)]
51. Hu, B.; Jin, J.; Guo, A.Y.; Zhang, H.; Luo, J.; Gao, G. GSDS 2.0: An upgraded gene feature visualization server. *Bioinformatics* **2015**, *31*, 1296–1297. [[CrossRef](#)]
52. Yu, C.P.; Lin, J.J.; Li, W.H. Positional distribution of transcription factor binding sites in *Arabidopsis thaliana*. *Sci. Rep.* **2016**, *6*, 25164. [[CrossRef](#)]
53. Lescot, M.; Déhais, P.; Thijs, G.; Rombauts, S. PlantCARE, a database of plant cis-acting regulatory elements and a portal to tools for in silico analysis of promoter sequences. *Nucleic Acids Res.* **2002**, *30*, 325–327. [[CrossRef](#)]
54. Fei, Z.; Je-Gun, J.; Tang, X. Tomato Functional Genomics Database: A comprehensive resource and analysis package for tomato functional genomics. *Nucleic Acids Res.* **2011**, *39*, 1156–1163. [[CrossRef](#)]
55. Kelman, A. The relationship of the pathogenicity of *Pseudomonas solanacearum* to colony appearance on a tetrazolium medium. *Phytopathology* **1954**, *44*, 693–695.
56. Lu, K.; Li, T.; He, J.; Chang, W.; Zhang, R.; Liu, M. qPrimerDB: A thermodynamics-based gene-specific qPCR primer database for 147 organisms. *Nucleic Acids Res.* **2018**, *46*, 1229–1236. [[CrossRef](#)]
57. Ding, X.; Li, J.; Pan, Y.; Zhang, Y.; Ni, L.; Wang, Y.; Zhang, X. Genome-wide identification and expression analysis of the UGLcAE gene family in tomato. *Int. J. Mol. Sci.* **2018**, *19*, 1583. [[CrossRef](#)]
58. Livak, K.J.; Schmittgen, T.D. Analysis of relative gene expression data using real-time quantitative PCR and the 2-DDCt method. *Methods* **2001**, *25*, 402–408. [[CrossRef](#)]
59. Le Berre, M.; Gerlach, J.Q.; Dziembała, I.; Kilcoyne, M. Calculating half maximal inhibitory concentration (IC50) values from glycomics microarray data using GraphPad Prism. *Methods Mol. Biol.* **2022**, *2460*, 89–111.
60. Lynch, M.; Conery, J.S. The evolutionary fate and consequences of duplicate genes. *Science* **2000**, *290*, 1151–1155. [[CrossRef](#)]
61. Blanc, G.; Wolfe, K.H. Widespread paleopolyploidy in model plant species inferred from age distributions of duplicate genes. *Plant Cell* **2004**, *16*, 1667–1678. [[CrossRef](#)]
62. Cheung, J.; Estivill, X.; Khaja, R.; MacDonald, J.R.; Lau, K.; Tsui, L.C.; Scherer, S.W. Genome-wide detection of segmental duplications and potential assembly errors in the human genome sequence. *Genome Biol.* **2003**, *4*, 25. [[CrossRef](#)] [[PubMed](#)]
63. Denny, T.P. *Ralstonia solanacearum*—A plant pathogen in touch with its host. *Trends Microbiol.* **2000**, *8*, 486–489. [[CrossRef](#)]

64. Mansfield, J.; Genin, S.; Magori, S.; Citovsky, V.; Sriariyanum, M.; Ronald, P.; Dow, M.; Verdier, V.; Beer, S.V.; Machado, M.A.; et al. Top 10 plant pathogenic bacteria in molecular plant pathology. *Mol. Plant Pathol.* **2012**, *13*, 614–629. [[CrossRef](#)]
65. Haider, M.S.; Kurjogi, M.M.; Khalil-Ur-Rehman, M.; Fiaz, M.; Pervaiz, T.; Jiu, S.; Haifeng, J.; Chen, W.; Fang, J. Grapevine immune signaling network in response to drought stress as revealed by transcriptomic analysis. *Plant Physiol. Biochem.* **2017**, *121*, 187–195. [[CrossRef](#)] [[PubMed](#)]
66. Kerk, D.; Bulgrien, J.; Smith, D.W.; Barsam, B.; Veretnik, S.; Gribskov, M. The complement of protein phosphatase catalytic subunits encoded in the genome of *Arabidopsis*. *Plant Physiol.* **2002**, *129*, 908–925. [[CrossRef](#)] [[PubMed](#)]
67. Djami-Tchatchou, A.T.; Maake, M.P.; Piater, L.A.; Dubery, I.A. Isonitrosoacetophenone drives transcriptional reprogramming in *Nicotiana tabacum* cells in support of innate immunity and defense. *PLoS ONE* **2015**, *10*, e0117377. [[CrossRef](#)] [[PubMed](#)]
68. Kim, S.; Park, M.; Yeom, S.I. Genome sequence of the hot pepper provides insights into the evolution of pungency in *Capsicum* species. *Nat. Genet.* **2014**, *46*, 270–278. [[CrossRef](#)]
69. Yang, Q.; Liu, K.; Niu, X.; Wang, Q.; Wan, Y.; Yang, F.; Li, G.; Wang, Y.; Wang, R. Genome-wide identification of PP2C genes and their expression profiling in response to drought and cold stresses in *Medicago truncatula*. *Sci. Rep.* **2018**, *8*, 12841. [[CrossRef](#)]
70. Fuchs, S.; Grill, E.; Meskiene, I.; Schweighofer, A. Type 2C protein phosphatases in plants. *FEBS J.* **2013**, *280*, 681–693. [[CrossRef](#)]
71. Moore, R.C.; Purugganan, M.D. The early stages of duplicate gene evolution. *Proc. Natl. Acad. Sci. USA* **2003**, *100*, 15682–15687. [[CrossRef](#)]
72. Juretic, N.; Hoen, D.R.; Huynh, M.L.; Harrison, P.M.; Bureau, T.E. The evolutionary fate of MULE-mediated duplications of host gene fragments in rice. *Genome Res.* **2005**, *15*, 1292–1297. [[CrossRef](#)]
73. Pervez, M.A.; Ayub, C.M.; Khan, H.A.; Shahid, M.A.; Ashraf, I. Effect of drought stress on growth, yield and seed quality of tomato (*Lycopersicon esculentum* L.). *Pak. J. Agric. Sci.* **2009**, *46*, 174–178.
74. Zhang, P.; Senge, M.; Dai, Y. Effects of salinity stress at different growth stages on tomato growth, yield, and water-use efficiency. *Commun. Soil Sci. Plant Anal.* **2017**, *48*, 624–634. [[CrossRef](#)]
75. Peleg, Z.; Blumwald, E. Hormone balance and abiotic stress tolerance in crop plants. *Curr. Opin. Plant Biol.* **2011**, *14*, 290–295. [[CrossRef](#)]
76. Rubio, S.; Rodrigues, A.; Saez, A.; Dizon, M.B.; Galle, A.; Kim, T.; Santiago, J.; Flexas, J.; Schroeder, J.I.; Rodriguez, P.L. Triple loss of function of protein phosphatases type 2C leads to partial constitutive response to endogenous abscisic acid. *Plant Physiol.* **2009**, *150*, 1345–1355. [[CrossRef](#)]
77. Saez, A.; Apostolova, N.; Gonzalez-Guzman, M.; Gonzalez-Garcia, M.P.; Nicolas, C.; Lorenzo, O.; Rodriguez, P.L. Gain-of-function and loss-of-function phenotypes of the protein phosphatase 2C HAB1 reveal its role as a negative regulator of abscisic acid signalling. *Plant J.* **2004**, *37*, 354–369. [[CrossRef](#)]
78. Sun, H.L.; Wang, X.J.; Ding, W.H.; Zhu, S.Y.; Zhao, R.; Zhang, Y.X.; Xin, Q.; Wang, X.F.; Zhang, D.P. Identification of an important site for function of the type2C protein phosphatase ABI2 in abscisic acid signalling in *Arabidopsis*. *J. Exp. Bot.* **2011**, *62*, 5713–5725. [[CrossRef](#)]
79. Allen, G.J.; Kuchitsu, K.; Chu, S.P.; Murata, Y.; Schroeder, J.I. *Arabidopsis* abi1-1 and abi2-1 phosphatase mutations reduce abscisic acid-induced cytoplasmic calcium rises in guard cells. *Plant Cell* **1999**, *11*, 1785–1798.
80. Kuhn, J.M.; Boisson-Dernier, A.; Dizon, M.B.; Maktabi, M.H.; Schroeder, J.I. The protein phosphatase AtPP2CA negatively regulates abscisic acid signal transduction in *Arabidopsis*, and effects of abh1 on AtPP2CA mRNA. *Plant Physiol.* **2006**, *140*, 127–139. [[CrossRef](#)]
81. Liu, X.; Zhu, Y.; Zhai, H.; Cai, H.; Ji, W.; Luo, X.; Li, J.; Bai, X. AtPP2CG1, a protein phosphatase 2C, positively regulates salt tolerance of *Arabidopsis* in abscisic acid-dependent manner. *Biochem. Biophys. Res. Commun.* **2012**, *422*, 710–715. [[CrossRef](#)]
82. Haider, M.S.; Kurjogi, M.M.; Khalil-Ur-Rehman, M. Drought stress revealed physiological, biochemical and gene-expressional variations in ‘Yoshihime’ peach (*Prunus persica* L.) cultivar. *J. Plant Interact.* **2018**, *13*, 83–90. [[CrossRef](#)]
83. Choopayak, C. *Characterization and Functional Analysis of a Novel PP2C Phosphatase AP2C2 from Arabidopsis*; University of Vienna: Vienna, Austria, 2008.
84. Chen, C.; Yu, Y.; Ding, X.; Liu, B.; Duanmu, H.; Zhu, D.; Sun, X.; Cao, L. Genome-wide analysis and expression profiling of PP2C clade D under saline and alkali stresses in wild soybean and *Arabidopsis*. *Protoplasma* **2017**, *255*, 643–654. [[CrossRef](#)]
85. Ali, M.; Javaid, A.; Naqvi, S.H.; Batcho, A.; Kayani, W.K.; Lal, A.; Sajid, I.A.; Nwogwugwu, J.O. Biotic stress triggered small RNA and RNAi defense response in plants. *Mol. Biol. Rep.* **2020**, *47*, 5511–5522. [[CrossRef](#)]
86. Atkinson, N.J.; Urwin, P.E. The interaction of plant biotic and abiotic stresses: From genes to the field. *J. Exp. Bot.* **2012**, *63*, 3523–3543. [[CrossRef](#)]
87. Suzuki, N.; Rivero, R.M.; Shulaev, V.; Blumwald, E.; Mittler, R. Abiotic and biotic stress combinations. *New Phytol.* **2014**, *203*, 32–43. [[CrossRef](#)]
88. Xiao, D.; Cui, Y.; Xu, F.; Xu, X.; Gao, G.; Wang, Y.; Guo, Z.; Wang, D.; Wang, N.N. Senescence-suppressed protein phosphatase directly interacts with the cytoplasmic domain of senescence-associated receptor-like kinase and negatively regulates leaf senescence in *Arabidopsis*. *Plant Physiol.* **2015**, *169*, 1275–1291. [[CrossRef](#)]
89. Li, Y.S.; Sun, H.; Wang, Z.F.; Duan, M.; Huang, S.D.; Yang, J.; Huang, J.; Zhang, H.S. A novel nuclear protein phosphatase 2C negatively regulated by ABL1 is involved in abiotic stress and panicle development in rice. *Mol. Biotechnol.* **2013**, *54*, 703–710. [[CrossRef](#)]

90. Li, W.; Cui, X.; Meng, Z.; Huang, X.; Xie, Q.; Wu, H.; Jin, H.; Zhang, D.; Liang, W. Transcriptional regulation of *Arabidopsis* MIR168a and ARGONAUTE1 homeostasis in ABA and abiotic stress responses. *Plant Physiol.* **2012**, *158*, 1279–1292. [[CrossRef](#)]
91. Maestrini, P.; Cavallini, A.; Rizzo, M.; Giordani, T.; Bernardi, R.; Durante, M.; Natali, L. Isolation and expression analysis of low temperature induced genes in white poplar (*Populus alba*). *Plant Physiol.* **2009**, *166*, 1544–1556. [[CrossRef](#)]
92. Wen, F.; Zhu, H.; Li, P.; Jiang, M.; Mao, W.; Ong, C.; Chu, Z. Genome-wide evolutionary characterization and expression analyses of WRKY family genes in *Brachypodium distachyon*. *DNA Res.* **2014**, *21*, 327–339. [[CrossRef](#)]